Journal of Computational Mathematics
Vol. 00, Pages 000–000 (XXXX)

An Asymptotic Preserving and Uniform Well-Balanced Scheme for the Isentropic Euler Equations with Gravitational Source Term

Farah Kanbar [1]
Christian Klingenberg [2]
Min Tang [3]

[1] University of Wuerzburg, Germany
Email address: kanbar.farah@gmail.com
[2] University of Wuerzburg, Germany
Email address: klingen@mathematik.uni-wuerzburg.de
[3] Shanghai Jiao Tong University, China
Email address: tangmin@sjtu.edu.cn.

Abstract. We propose an asymptotic preserving (AP) and well-balanced (WB) scheme for the isentropic compressible Euler system with gravitational source term. When the Mach number becomes small, the compressible Euler equation with gravitational source term converges to an incompressible Euler equation with spatial dependent density. We achieve AP by modifying the source term by adding and subtracting a term that includes the equilibrium information. The WB property is attained by introducing a very special spatial discretization to the stiff source terms. The proposed scheme can achieve both AP and WB properties. It is important to note that the WB property is independent of Mach number, i.e. WB property holds for all Mach number. A list of numerical test cases is added at the end to validate the robustness and the accuracy of the scheme compared to the recent literature.

Keywords. Asymptotic preserving, well balancing, MAC, low Mach.
2020 Mathematics Subject Classification. 65N06; 35B40; 76M45 .

1. Introduction

The non-dimensionalized Isentropic Euler equations with gravitational source term is given by,

$$\begin{aligned} \partial_t \rho + \nabla \cdot (\rho \mathbf{u}) &= 0, \\ \partial_t (\rho \mathbf{u}) + \nabla \cdot (\rho \mathbf{u} \otimes \mathbf{u}) + \frac{1}{\varepsilon^2} \nabla p(\rho) &= -\frac{1}{\varepsilon^2} \rho \nabla \phi. \end{aligned} \tag{1.1}$$

Here ρ is the density, $\mathbf{u}$ is the velocity field, p is the pressure. The pressure law is given by $p(\rho) = A\rho^\gamma$, where A and γ are positive constants. $\phi(x)$ is a given function representing the space dependent gravitational potential. ε is the ratio of the characteristic fluid velocity and the typical sound speed $\varepsilon^2 = \frac{|u|^2}{c^2}$. ε is referred to as "Mach number" and can be at $O(1)$ or very small.

When ε is very small, (1.1) is at the low Mach number regime, the pressure and gravity terms become stiff. The existence and uniqueness of solution to equation (1.1) can be found in the literature [9], [4]. It is proved rigorously in that when $\varepsilon \to 0$, solution to (1.1) converges to the solution of an incompressible equation. We give the formal derivation in the subsequent part. Moving the gravitational source term to the left-hand side of the second equation of (1.1) and using the pressure law, we then write (1.1) as,

$$\begin{aligned} \partial_t \rho + \nabla \cdot (\rho \mathbf{u}) &= 0, \\ \partial_t (\rho \mathbf{u}) + \nabla \cdot (\rho \mathbf{u} \otimes \mathbf{u}) + \frac{1}{\varepsilon^2} \rho \nabla W &= 0, \end{aligned} \tag{1.2}$$

The first author was supported by the National Center for Scientific Research CNRS-L.

with

$$W = \frac{A\gamma}{\gamma - 1}\rho^{\gamma-1} + \phi. \tag{1.3}$$

Assume that the Chapman-Enskog asymptotic expansions of the variables are,

$$\begin{aligned}\rho &= \rho^{(0)} + \varepsilon\rho^{(1)} + \varepsilon^2\rho^{(2)} + ...\\ \mathbf{u} &= \mathbf{u}^{(0)} + \varepsilon\mathbf{u}^{(1)} + \varepsilon^2\mathbf{u}^{(2)} + ...\\ W &= W^{(0)} + \varepsilon W^{(1)} + \varepsilon^2 W^{(2)} + ...\end{aligned}$$

The expansion of $\rho\nabla W$ can be seen as,

$$\begin{aligned}\rho\nabla W &= (\rho^{(0)} + \varepsilon\rho^{(1)} + \varepsilon^2\rho^{(2)} + \cdots)\nabla(W^{(0)} + \varepsilon W^{(1)} + \varepsilon^2 W^{(2)} + \cdots),\\ &= \rho^{(0)}\nabla W^{(0)} + \varepsilon\Big(\rho^{(0)}\nabla W^{(1)} + \rho^{(1)}\nabla W^{(0)}\Big) + \varepsilon^2\Big(\rho^{(0)}\nabla W^{(2)} + \rho^{(1)}\nabla W^{(1)} + \rho^{(2)}\nabla W^{(0)}\Big) + \cdots.\end{aligned} \tag{1.4}$$

Comparing the $\mathcal{O}(\frac{1}{\varepsilon^2})$ terms in system (1.2) and using $\rho^{(0)} \neq 0$, one deduces that $\nabla W^{(0)} = 0$. Then looking at the $\mathcal{O}(\frac{1}{\varepsilon})$ terms yields $\nabla W^{(1)} = 0$. From the definition of W in (1.3), $\nabla W^{(0)} = 0$ leads to,

$$\frac{A\gamma}{\gamma - 1}\big(\rho^{(0)}\big)^{\gamma-1} + \phi(x) = const$$

with *const* being a constant independent of x. Then

$$\big(\rho^{(0)}\big)^{\gamma-1} + \frac{\gamma - 1}{A\gamma}\phi(x) = const.$$

In the model (1.1), for a constant independent of x, $\phi(x)$ and $\phi(x) + const$ provide the same solution. Thus one can define a new $\tilde{\phi}(x) = \phi(x) + const$ such that $\big(\rho^{(0)}\big)^{\gamma-1} + \frac{\gamma-1}{A\gamma}\phi(x) = 1$. In the subsequent part, we drop the tilde above $\tilde{\phi}(x)$ and let

$$\rho^{(0)} = \left(1 - \frac{\gamma - 1}{\gamma A}\phi(x)\right)^{\frac{1}{\gamma-1}}, \tag{1.5}$$

which indicates that when $\varepsilon \ll 1$, $\rho^{(0)}$ becomes stationary.

To find the equation that $\mathbf{u}^{(0)}$ satisfies, we consider the $\mathcal{O}(1)$ terms in system (1.2) such that

$$\begin{aligned}&\partial_t\rho^{(0)} + \nabla\cdot(\rho^{(0)}\mathbf{u}^{(0)}) = 0,\\ &\partial_t(\rho^{(0)}\mathbf{u}^{(0)}) + \nabla\cdot(\rho^{(0)}\mathbf{u}^{(0)}\otimes\mathbf{u}^{(0)}) + \rho^{(0)}\nabla W^{(2)} + \rho^{(1)}\nabla W^{(1)} + \rho^{(2)}\nabla W^{(0)} = 0.\end{aligned} \tag{1.6}$$

Using $\nabla W^{(0)} = \nabla W^{(1)} = 0$, system (1.6) can be written as

$$\begin{aligned}&\nabla\cdot(\rho^{(0)}\mathbf{u}^{(0)}) = 0,\\ &\partial_t\mathbf{u}^{(0)} + \mathbf{u}^{(0)}\nabla\cdot\mathbf{u}^{(0)} + \nabla W^{(2)} = 0.\end{aligned} \tag{1.7}$$

(1.7) is the incompressible isentropic Euler equations.

When ε goes to zero in (1.1), the sound speed is fast, and classical shock capturing schemes require very small time steps. Hence, asymptotic preserving (AP) schemes that allow large space and time steps become popular in this area. A numerical scheme is AP if when the scaling parameter goes to the limit in the discretized scheme, it converges to a good discretization of the corresponding limit model. The main advantage of AP schemes is that their stability and convergence are independent of the stiffness of the equation. AP schemes usually discretize the stiff terms implicitly, which leads to an IMEX(Implicit-Explicit) discretization of the model [16]. The space discretization is important as well due to the special structure of the limiting incompressible equation. Developing AP schemes

for compressible fluid equations in their incompressible limits is a well-studied topic in computational fluid dynamics. A list of these schemes is listed here [1, 6, 20, 11, 14, 7, 8, 15, 19, 2, 22, 21].

The hydrostatic steady state is that the velocity is zero, and the pressure exactly balances the gravitational force. As has been discussed in [17], this steady state is of particular interest for the Euler equations with gravitation. The dynamics when the solution is close to the hydrostatic steady state are important in the simulation of waves in stellar atmospheres [3] or some numerical weather prediction [10]. To get the dynamics of small perturbations near the equilibrium, the ratio between the magnitude of the truncation errors and the perturbations has to be small enough, which is too expensive for standard schemes. To overcome this challenge, it is of interest to have a numerical scheme that maintains discrete stationary solutions up to machine precision [17]. This is so-called the well-balanced property and well-balanced (WB) schemes can effectively resolve small perturbations of the steady state of interest. For the Euler equation with gravity source term, several strategies have been proposed to achieve the WB property [17, 5, 13], in which complicated modifications of the fluxes taking into account the source term are usually employed.

In this paper, we extend the AP finite difference staggered approach for the isentropic Euler equation, to (1.1) with gravity source term. On the one hand, when $\phi(x) \equiv 0$, we want the scheme to be the same as the one suggested by Goudon et al. in [11], on the other hand, we aim to get an AP scheme when $\phi(x)$ is not uniform in space. However, it is not easy to achieve these two requirements at the same time. First of all, the density $\rho^{(0)}$ in (1.5) is space-dependent, it is obtained by the balancing between the pressure term $\nabla p(\rho)$ and the gravity term $\rho\nabla\phi$. But the strategies of achieving AP properties in [11, 14, 7, 8] usually split the pressure term into two parts and treat them differently, which will break down the balance. Therefore, if keep using the same splitting strategy on the left-hand side of (1.1), one has to design another balance that can provide the space-dependent limiting density. We modify the source term by adding and subtracting a term that includes the equilibrium information. Proper implicit and explicit treatments of these two additional terms provide a new balance that gives the space nonuniform equilibrium. Secondly, one has to carefully design the spatial discretization due to the following two apparently opposite observations: 1) when $\phi(x) \equiv 0$, (1.1) becomes a conservative hyperbolic system, the discretization for the left-hand side of (1.1) has to be conservative; 2) in the formal derivation of the incompressible limit equation, one has to first reformulate (1.1) into (1.2) which is a non-conservative form even if $\phi \equiv 1$. We solve this difficulty by introducing a very special spatial discretization for the stiff source terms. Since this spatial discretization preserves exactly the discrete hydrostatic steady state, it not only achieves AP but also gives the WB property of the scheme.

The new contributions of the current work are that: 1) It provides a strategy of extending the AP schemes designed for the isentropic Euler system to the case with gravity source term, without changing the code for the hyperbolic part; 2) It can achieve not only AP but also WB. It is important to note that the WB property is independent of Mach number ε, i.e. WB property holds for all ε. As far as we know, our scheme is the first scheme that can achieve both properties *uniform in* ϵ for an isentropic Euler system with a gravity source term.

The organization of the paper is as follows. A detailed description of the method can be found in section 2. We show both AP and SP properties of the proposed scheme in 3. The robustness of the scheme and its AP and SP properties are tested via a collection of numerical test cases from the literature in section 4. Concluding remarks and possible future extensions are mentioned in section 5.

2. The Two-dimensional Numerical Scheme

2.1. The semi-discrete scheme

Similar as in [14] and [11], we split the divergence in the density equation as well as the pressure and the gravitational source term in the momentum equation. Let

$$\rho_0 = \left(1 - \frac{\gamma-1}{\gamma A}\phi(x)\right)^{\frac{1}{\gamma-1}}. \tag{2.1}$$

The system (1.1) is splitted into the following two subsystems:

$$\begin{aligned} &\partial_t \rho + \alpha \nabla \cdot (\rho \mathbf{u}) = 0, \\ &\partial_t(\rho \mathbf{u}) + \nabla \cdot (\rho \mathbf{u} \otimes \mathbf{u}) + \frac{1}{\varepsilon^2}\nabla\left[p(\rho) - a(t)\rho\right] = -\frac{1}{\varepsilon^2}\rho\nabla\phi - \frac{a(t)}{\varepsilon^2}\rho\nabla \ln \rho_0, \end{aligned} \tag{2.2}$$

and

$$\begin{aligned} &\partial_t \rho + (1-\alpha)\nabla \cdot (\rho \mathbf{u}) = 0, \\ &\partial_t(\rho \mathbf{u}) + \frac{1}{\varepsilon^2}a(t)\nabla\rho = \frac{a(t)}{\varepsilon^2}\rho\nabla \ln \rho_0. \end{aligned} \tag{2.3}$$

where $\mathbf{u} = (u, v)^T$, $0 \le \alpha < 1$ is a constant and the time dependent function $a(t) > 0$ depends on the hyperbolicity of the system (2.2). The choices of the terms $\frac{1}{\varepsilon^2}\nabla a(t)\rho$ in the pressure component and $\frac{1}{\varepsilon^2}a(t)\rho\nabla \ln \rho_0$ in the source term are related to the fact that the leading order $\rho^{(0)}$ has the form as in (1.5). When there is no gravity, i.e. $\rho_0 \equiv 1$, the modification becomes the same as in [11]. We will see the necessity of this modification in the AP proof later on.

The first system (2.2) takes into account the slow speed, while the second part (2.3) considers the fast sound wave. Similar as discussed in [11], numerical viscosity will be added in the first system but not the second.

In the conservative form, (2.2) can be written as

$$U_t + F(U)_x + G(U)_y = S(U), \tag{2.4}$$

with

$$U = \begin{pmatrix} \rho \\ \rho u \\ \rho v \end{pmatrix}, \qquad F(U) = \begin{pmatrix} \alpha\rho u \\ \rho u^2 + \frac{p(\rho)-a(t)\rho}{\varepsilon^2} \\ \rho uv \end{pmatrix},$$

$$G(U) = \begin{pmatrix} \alpha\rho v \\ \rho uv \\ \rho v^2 + \frac{p(\rho)-a(t)\rho}{\varepsilon^2} \end{pmatrix}, \quad S(U) = \begin{pmatrix} 0 \\ -\frac{1}{\varepsilon^2}\rho\phi_x - \frac{a(t)}{\varepsilon^2}\rho(\ln\rho_0)_x \\ -\frac{1}{\varepsilon^2}\rho\phi_y - \frac{a(t)}{\varepsilon^2}\rho(\ln\rho_0)_y \end{pmatrix}.$$

The eigenvalues of the jacobian matrix of $F(U)$ are

$$\lambda_1 = u, \quad \lambda_2 = u + c, \quad \lambda_3 = u - c, \quad \text{with} \quad c(\rho, u) = \sqrt{(1-\alpha)u^2 + \alpha\frac{p'(\rho) - a(t)}{\varepsilon^2}}.$$

Similar calculations hold for $G(U)$, the flux along y. The choice of $a(t)$ is to guarantee the hyperbolicity of the system (2.2). We choose $a(t)$ such that the eigenvalues of the jacobian matrices of $F(U)$, $G(U)$ are real and positive i.e. $p'(\rho) \ge a(t)$. Hence, $a(t)$ is chosen as the following,

$$a_0(t) = \min_x \left\{p'(\rho)\right\}. \tag{2.5}$$

But, with this choice, spurious oscillations are observed in some test cases for large values of ε. They appear in regions where the density is nearly uniform and the material velocity vanishes. Indeed, in these regions, the corresponding sound speed vanishes and the spurious oscillations are due to

a lack of numerical viscosity in the slow dynamic part of the splitting. Therefore, as in [11], let $a(t) = (1-\varepsilon^2)\min_x \{p'(\rho)\}$, for $\varepsilon < 1$. This $a(t)$ can eliminates the spurious oscillations that might appear for large ε. For more details, see [11].

Let Δt be the time step, $t^0 = 0$, and for a positive integer n, we set $t^{n+1} = t^n + \Delta t$. The two subsystems (2.2), (2.3) can now be discretized as,

$$\begin{cases} \frac{\rho^* - \rho^n}{\Delta t} + \alpha \nabla \cdot (\rho \mathbf{u})^n = 0, \\ \frac{(\rho \mathbf{u})^* - (\rho \mathbf{u})^n}{\Delta t} + \nabla \cdot (\rho \mathbf{u} \otimes \mathbf{u})^n + \frac{1}{\varepsilon^2} \nabla \left[p(\rho) - a(t)\rho\right]^n = -\frac{1}{\varepsilon^2} \rho^n \nabla \phi - \frac{a^n}{\varepsilon^2} \rho^n \nabla \ln \rho_0, \end{cases} \tag{2.6}$$

and

$$\begin{cases} \frac{\rho^{n+1} - \rho^*}{\Delta t} + (1-\alpha) \nabla \cdot (\rho \mathbf{u})^{n+1} = 0, \\ \frac{(\rho \mathbf{u})^{n+1} - (\rho \mathbf{u})^*}{\Delta t} + \frac{1}{\varepsilon^2} a(t^n) \nabla \rho^{n+1} = \frac{a^n}{\varepsilon^2} \rho^{n+1} \nabla \ln \rho_0. \end{cases} \tag{2.7}$$

The above two semi-discretization (2.6) and (2.7) yield an IMEX discretization

$$\begin{aligned} &\frac{\rho^{n+1} - \rho^n}{\Delta t} + \alpha \nabla \cdot (\rho \mathbf{u})^n + (1-\alpha) \nabla \cdot (\rho \mathbf{u})^{n+1} = 0, \\ &\frac{(\rho \mathbf{u})^{n+1} - (\rho \mathbf{u})^n}{\Delta t} + \nabla \cdot (\rho \mathbf{u} \otimes \mathbf{u})^n + \frac{1}{\varepsilon^2} \nabla \left[p(\rho) - a(t)\rho\right]^n + \frac{1}{\varepsilon^2} a(t) \nabla \rho^{n+1} \\ &\qquad = -\frac{1}{\varepsilon^2} \rho^n \nabla \phi - \frac{a(t)}{\varepsilon^2} \rho^n \nabla \ln \rho_0 + \frac{a(t)}{\varepsilon^2} \rho^{n+1} \nabla \ln \rho_0. \end{aligned} \tag{2.8}$$

2.2. **The fully-discrete scheme**

For spatial discretization, we use the staggered method proposed in [11], [12]. Staggered schemes are proven to be very efficient for incompressible flows simulations. We consider a computational domain $[x_L, x_R] \times [y_L, y_R]$ and Cartesian 2D grid points. The grid points are x_i, y_j for $i, j \in \{1, ..., N_x\}$ and $j \in \{1, ..., N_y\}$ and we define $x_{i+\frac{1}{2}} = \frac{x_i + x_{i+1}}{2}$ and $y_{j+\frac{1}{2}} = \frac{y_j + y_{j+1}}{2}$ for $i \in \{1, ..., N_x - 1\}$, $j \in \{1, ..., N_y - 1\}$. Let $\Delta x_i, \Delta x_{i+\frac{1}{2}}, \Delta y_j$, and $\Delta y_{j+\frac{1}{2}}$ be respectively the length of the interval $[x_{i-\frac{1}{2}}, x_{i+\frac{1}{2}}]$, $[x_i, x_{i+1}]$, $[y_{j-\frac{1}{2}}, y_{j+\frac{1}{2}}]$ and $[y_j, y_{j+1}]$. In our calculations, we set $\Delta x_i = \Delta x_{i+\frac{1}{2}} = x$ and $\Delta y_j = \Delta y_{j+\frac{1}{2}} = \Delta y$.

As in Figure 1, the density ρ is defined at the points $(x_{i+\frac{1}{2}}, y_{j+\frac{1}{2}})$, while the velocity u in the x-direction is evaluated on the points $(x_i, y_{j+\frac{1}{2}})$ and the velocity v in the y-direction is evaluated on the points $(x_{i+\frac{1}{2}}, y_j)$. The density on the edges of the primal mesh can be defined by the average value of two neighbouring cells such that

$$\begin{aligned} \rho_{i,j+\frac{1}{2}} &= \frac{\rho_{i+\frac{1}{2},j+\frac{1}{2}} + \rho_{i-\frac{1}{2},j+\frac{1}{2}}}{2}, \\ \rho_{i+\frac{1}{2},j} &= \frac{\rho_{i+\frac{1}{2},j+\frac{1}{2}} + \rho_{i+\frac{1}{2},j-\frac{1}{2}}}{2}. \end{aligned}$$

The numerical solution is evolved on the staggered grid and the fluxes are defined as in [11]. We start

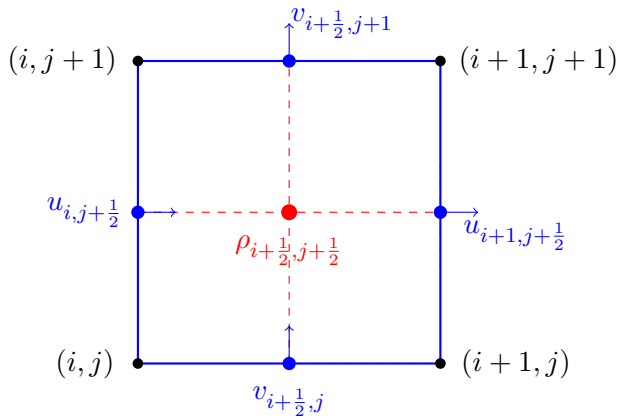

FIGURE 1. MAC discretization.

by presenting a discretization for the slow explicit system (2.6),

$$\begin{cases} \frac{\rho^*_{i+\frac{1}{2},j+\frac{1}{2}}-\rho^n_{i+\frac{1}{2},j+\frac{1}{2}}}{\Delta t}+\alpha\left[\frac{F^{x,n}_{i+1,j+\frac{1}{2}}-F^{x,n}_{i,j+\frac{1}{2}}}{\Delta x}+\frac{F^{y,n}_{i+\frac{1}{2},j+1}-F^{y,n}_{i+\frac{1}{2},j}}{\Delta y}\right]=0, \\ \frac{\rho^*_{i,j+\frac{1}{2}}u^*_{i,j+\frac{1}{2}}-\rho^n_{i,j+\frac{1}{2}}u^n_{i,j+\frac{1}{2}}}{\Delta t}+\frac{\zeta^{u,x}_{i+\frac{1}{2},j+\frac{1}{2}}-\zeta^{u,x}_{i-\frac{1}{2},j+\frac{1}{2}}}{\Delta x}+\frac{\zeta^{u,y}_{i,j+1}-\zeta^{u,y}_{i,j}}{\Delta y} \\ +\frac{1}{\varepsilon^2}\frac{\Pi^n_{i+\frac{1}{2},j+\frac{1}{2}}-\Pi^n_{i-\frac{1}{2},j+\frac{1}{2}}}{\Delta x}=-\frac{\rho^n_{i,j+\frac{1}{2}}}{\varepsilon^2\rho_{0,i,j+\frac{1}{2}}}\frac{P(\rho_{0,i+\frac{1}{2},j+\frac{1}{2}})-P(\rho_{0,i-\frac{1}{2},j+\frac{1}{2}})}{\Delta x}-\frac{a^n_d\rho^n_{i,j+\frac{1}{2}}}{\varepsilon^2\rho_{0,i,j+\frac{1}{2}}}\frac{\rho_{0,i+\frac{1}{2},j+\frac{1}{2}}-\rho_{0,i-\frac{1}{2},j+\frac{1}{2}}}{\Delta x}, \\ \frac{\rho^*_{i+\frac{1}{2},j}v^*_{i+\frac{1}{2},j}-\rho^n_{i+\frac{1}{2},j}v^n_{i+\frac{1}{2},j}}{\Delta t}+\frac{\zeta^{v,x}_{i+1,j}-\zeta^{v,x}_{i,j}}{\Delta x}+\frac{\zeta^{v,y}_{i+\frac{1}{2},j+\frac{1}{2}}-\zeta^{v,y}_{i+\frac{1}{2},j-\frac{1}{2}}}{\Delta y} \\ +\frac{1}{\varepsilon^2}\frac{\Pi^n_{i+\frac{1}{2},j+\frac{1}{2}}-\Pi^n_{i+\frac{1}{2},j-\frac{1}{2}}}{\Delta y}=-\frac{\rho^n_{i+\frac{1}{2},j}}{\varepsilon^2\rho_{0,i+\frac{1}{2},j}}\frac{P(\rho_{0,i+\frac{1}{2},j+\frac{1}{2}})-P(\rho_{0,i+\frac{1}{2},j-\frac{1}{2}})}{\Delta y}-\frac{a^n_d\rho^n_{i+\frac{1}{2},j}}{\varepsilon^2\rho_{0,i+\frac{1}{2},j}}\frac{\rho_{0,i+\frac{1}{2},j+\frac{1}{2}}-\rho_{0,i+\frac{1}{2},j-\frac{1}{2}}}{\Delta y}. \end{cases} \tag{2.9}$$

with

$$\Pi^n_{i+\frac{1}{2},j+\frac{1}{2}}=P\big(\rho^n_{i+\frac{1}{2},j+\frac{1}{2}}\big)-a^n_d\rho^n_{i+\frac{1}{2},j+\frac{1}{2}}$$

where a^n_d is the discrete version of $a(t)$ defined as,

$$a^n_d=(1-\varepsilon^2)\min_{i,j}\left\{P'(\rho^n_{i+\frac{1}{2},j+\frac{1}{2}})\right\}.$$

The flux terms are

$$F^x_{i,j+\frac{1}{2}}=F^{x,+}_{i,j+\frac{1}{2}}+F^{x,-}_{i,j+\frac{1}{2}}=F^+(\rho_{i-\frac{1}{2},j+\frac{1}{2}},u_{i,j+\frac{1}{2}})+F^-(\rho_{i+\frac{1}{2},j+\frac{1}{2}},u_{i,j+\frac{1}{2}}),$$
$$F^y_{i+\frac{1}{2},j}=F^{y,+}_{i+\frac{1}{2},j}+F^{y,-}_{i+\frac{1}{2},j}=F^+(\rho_{i+\frac{1}{2},j-\frac{1}{2}},v_{i+\frac{1}{2},j})+F^-(\rho_{i+\frac{1}{2},j+\frac{1}{2}},v_{i+\frac{1}{2},j}),$$

$$\zeta^{u,x}_{i+\frac{1}{2},j+\frac{1}{2}}=u_{i,j+\frac{1}{2}}F^{x,+}_{i+\frac{1}{2},j+\frac{1}{2}}+u_{i+1,j+\frac{1}{2}}F^{x,+}_{i+\frac{1}{2},j+\frac{1}{2}},\qquad \zeta^{u,y}_{i,j}=u_{i,j-\frac{1}{2}}F^{y,+}_{i,j}+u_{i,j+\frac{1}{2}}F^{y,+}_{i,j}$$

$$\zeta^{v,x}_{i,j}=v_{i-\frac{1}{2},j}F^{x,+}_{i,j}+v_{i+\frac{1}{2},j}F^{x,+}_{i,j},\qquad \zeta^{v,y}_{i+\frac{1}{2},j+\frac{1}{2}}=v_{i+\frac{1}{2},j}F^{y,+}_{i+\frac{1}{2},j+\frac{1}{2}}+v_{i+\frac{1}{2},j+1}F^{y,+}_{i+\frac{1}{2},j+\frac{1}{2}}$$

with

$$F^+(\rho,u)=\begin{cases}0, & \text{if} \quad u\le -c(\rho,u),\\ \frac{\rho}{4c(\rho,u)}(v+c(\rho,u))^2, & \text{if} \quad |u|\le c(\rho,u),\\ \rho u, & \text{if} \quad u\ge c(\rho,u),\end{cases}$$

$$F^-(\rho,u)=\begin{cases}\rho u, & \text{if} \quad u\le -c(\rho,u),\\ -\frac{\rho}{4c(\rho,u)}(v-c(\rho,u))^2, & \text{if} \quad |u|\le c(\rho,u),\\ 0, & \text{if} \quad u\ge c(\rho,u),\end{cases}$$

and

$$F^{x,\pm}_{i+\frac12,j+\frac12}=\frac12\left(F^{x,\pm}_{i,j+\frac12}+F^{x,\pm}_{i+1,j+\frac12}\right),\qquad F^{y,\pm}_{i,j}=\frac12\left(F^{y,\pm}_{i+\frac12,j}+F^{y,\pm}_{i-\frac12,j}\right).$$

In (2.9), from the definition of ρ_0 in (1.5), one has

$$\frac{1}{\rho_{0,i,j+\frac12}}\frac{P(\rho_{0,i+\frac12,j+\frac12})-P(\rho_{0,i-\frac12,j+\frac12})}{\Delta x}\approx\nabla\phi, \tag{2.10}$$

$$\frac{1}{\rho_{0,i,j+\frac12}}\frac{\rho_{0,i+\frac12,j+\frac12}-\rho_{0,i-\frac12,j+\frac12}}{\Delta x}\approx\partial_x\ln\rho_0, \tag{2.11}$$

$$\frac{1}{\rho_{0,i+\frac12,j}}\frac{\rho_{0,i+\frac12,j+\frac12}-\rho_{0,i+\frac12,j-\frac12}}{\Delta y}\approx\partial_y\ln\rho_0 \tag{2.12}$$

These specific discrete forms are crucial for the AP and WB properties of the fully discretized scheme. We will see their benifits in section 3.

The next step is to discretize the implicit system (2.7) for fast sound wave by

$$\begin{cases}\frac{\rho^{n+1}_{i+\frac12,j+\frac12}-\rho^{*}_{i+\frac12,j+\frac12}}{\Delta t}\\ +(1-\alpha)\Big[\frac{(F^{n+1})^{Up,x}_{i+1,j+\frac12}-(F^{n+1})^{Up,x}_{i,j+\frac12}}{\Delta x}+\frac{(F^{n+1})^{Up,y}_{i+\frac12,j+1}-(F^{n+1})^{Up,y}_{i+\frac12,j}}{\Delta y}\Big]=0,\\ \frac{\rho^{n+1}_{i,j+\frac12}u^{n+1}_{i,j+\frac12}-\rho^{*}_{i,j+\frac12}u^{*}_{i,j+\frac12}}{\Delta t}\\ +\frac{a^n_d}{\varepsilon^2}\frac{\rho^{n+1}_{i+\frac12,j+\frac12}-\rho^{n+1}_{i-\frac12,j+\frac12}}{\Delta x}=\frac{a^n_d\rho^{n+1}_{i,j+\frac12}}{\varepsilon^2\rho^{n+1}_{0,i,j+\frac12}}\frac{\rho_{0,i+\frac12,j+\frac12}\rho_{0,i-\frac12,j+\frac12}}{\Delta x},\\ \frac{\rho^{n+1}_{i+\frac12,j}v^{n+1}_{i+\frac12,j}-\rho^{*}_{i+\frac12,j}v^{*}_{i+\frac12,j}}{\Delta t}\\ +\frac{a^n_d}{\varepsilon^2}\frac{\rho^{n+1}_{i+\frac12,j+\frac12}-\rho^{n+1}_{i+\frac12,j-\frac12}}{\Delta y}=\frac{a^n_d\rho^{n+1}_{i+\frac12,j}}{\varepsilon^2\rho^{n+1}_{0,i+\frac12,j}}\frac{\rho_{0,i+\frac12,j+\frac12}-\rho_{0,i+\frac12,j-\frac12}}{\Delta y},\end{cases} \tag{2.13}$$

where $(F^{n+1})^{Up,x}_{i,j+\frac12}$ and $(F^{n+1})^{Up,y}_{i+\frac12,j}$ are the upwind fluxes defined as following,

$$\begin{aligned}(F^{n+1})^{Up,x}_{i,j+\frac12}&=\rho^{n+1}_{i-\frac12,j+\frac12}\left[u^{n+1}_{i,j+\frac12}\right]^+-\rho^{n+1}_{i+\frac12,j+\frac12}\left[u^{n+1}_{i,j+\frac12}\right]^-\\ (F^{n+1})^{Up,y}_{i+\frac12,j}&=\rho^{n+1}_{i+\frac12,j-\frac12}\left[v^{n+1}_{i+\frac12,j}\right]^+-\rho^{n+1}_{i+\frac12,j+\frac12}\left[v^{n+1}_{i+\frac12,j}\right]^-.\end{aligned} \tag{2.14}$$

Here $[\cdot]^+=\max\{\cdot,0\}$ and $[\cdot]^-=-\min\{\cdot,0\}$ represents respectively the positive and negative parts of the given function. The fast implicit part is solved via solving an elliptic equation of ρ. From the last

two equations in (2.13), $u^{n+1}_{i,j+\frac{1}{2}}$ and $v^{n+1}_{i+\frac{1}{2},j}$ can be written as a function of ρ^{n+1} such that

$$u^{n+1}_{i,j+\frac{1}{2}} = \frac{1}{\rho^{n+1}_{i,j+\frac{1}{2}}}\left[\rho^{*}_{i,j+\frac{1}{2}}u^{*}_{i,j+\frac{1}{2}} - \frac{a^n_d\Delta t}{\varepsilon^2}\frac{\rho^{n+1}_{i+\frac{1}{2},j+\frac{1}{2}} - \rho^{n+1}_{i-\frac{1}{2},j+\frac{1}{2}}}{\Delta x} + \frac{a^n_d\Delta t}{\varepsilon^2}\frac{\rho^{n+1}_{i,j+\frac{1}{2}}}{\rho_{0,i,j+\frac{1}{2}}}\frac{\rho_{0,i+\frac{1}{2},j+\frac{1}{2}} - \rho_{0,i-\frac{1}{2},j+\frac{1}{2}}}{\Delta x}\right], \tag{2.15}$$

and

$$v^{n+1}_{i+\frac{1}{2},j} = \frac{1}{\rho^{n+1}_{i+\frac{1}{2},j}}\left[\rho^{*}_{i+\frac{1}{2},j}v^{*}_{i+\frac{1}{2},j} - \frac{a^n_d\Delta t}{\varepsilon^2}\frac{\rho^{n+1}_{i+\frac{1}{2},j+\frac{1}{2}} - \rho^{n+1}_{i+\frac{1}{2},j-\frac{1}{2}}}{\Delta y} + \frac{a^n_d\Delta t}{\varepsilon^2}\frac{\rho^{n+1}_{i+\frac{1}{2},j}}{\rho_{0,i+\frac{1}{2},j}}\frac{\rho_{0,i+\frac{1}{2},j+\frac{1}{2}} - \rho_{0,i+\frac{1}{2},j-\frac{1}{2}}}{\Delta y}\right]. \tag{2.16}$$

By substitute the above two equations into the density equation in (2.13), then we solve the system by Newton-Raphson method.

3. The AP and WB properties of the scheme

3.1. The AP property of the semi-discretized scheme

In order to prove the AP property of the semi-discrete scheme we need to prove that as ε goes to zero, (2.8) is a good discretization of the incompressible limit equation (1.7).

We reformulate the momentum equation in (2.8) before the expansion, as at the PDE level. Let

$$M(\rho) = \int_q^\rho \frac{1}{\rho'}d\rho', \qquad N(\rho) = \int_q^\rho A\gamma(\rho')^{\gamma-2}d\rho' \tag{3.1}$$

with $q > 0$ being a constant independent of ρ.

We then write the last two terms on the left hand side and the right hand side of the momentum equation in (2.8), into the multiplication of ρ and a term of divergence form:

- The two terms involving ρ^{n+1}.

$$\frac{1}{\varepsilon^2}a^n\nabla\rho^{n+1} - \frac{a^n}{\varepsilon^2}\rho^{n+1}\nabla\ln\rho_0 = \frac{a^n}{\varepsilon^2}\left[\nabla\rho^{n+1} - \rho^{n+1}\nabla\ln\rho_0\right] = \frac{a^n}{\varepsilon^2}\rho^{n+1}\left[\nabla M(\rho^{n+1}) - \nabla\ln\rho_0\right].$$

  The last equality holds due to the definition of $M(\rho)$ in (3.1).

- The two terms involving ρ^n.

$$\begin{aligned}
&\frac{1}{\varepsilon^2}\nabla\left[p(\rho) - a(t)\rho\right]^n + \frac{1}{\varepsilon^2}\rho^n\nabla\phi + \frac{a^n}{\varepsilon^2}\rho^n\nabla\ln\rho_0\\
=&\frac{1}{\varepsilon^2}\left[\gamma A(\rho^n)^{\gamma-1}\nabla\rho^n - a^n\nabla\rho^n + a^n\rho^n\nabla\ln\rho_0 + \rho^n\nabla\phi\right],\\
=&\frac{1}{\varepsilon^2}\rho^n\left[\gamma A(\rho^n)^{\gamma-2}\nabla\rho^n + \nabla\phi - a^n\frac{\nabla\rho^n}{\rho^n} + a^n\nabla\ln\rho_0\right],\\
=&\frac{1}{\varepsilon^2}\rho^n\left[\nabla N(\rho^n) + \nabla\phi - a^n[\nabla M(\rho^n) - \nabla\ln\rho_0]\right].
\end{aligned}$$

  The last equality holds due to the definitions of $N(\rho)$ and $M(\rho)$ in (3.1).

Hence, the momentum equation can be rewritten as,

$$\begin{aligned}
\frac{(\rho\mathbf{u})^{n+1} - (\rho\mathbf{u})^n}{\Delta t} + \nabla\cdot(\rho\mathbf{u}\otimes\mathbf{u})^n + \frac{1}{\varepsilon^2}\rho^n\Big[&\nabla N(\rho^n) + \nabla\phi\\
&- a^n[\nabla M(\rho^n) - \nabla\ln\rho_0]\Big] + \frac{a^n}{\varepsilon^2}\rho^{n+1}\left[\nabla M(\rho^{n+1}) - \nabla\ln\rho_0\right] = 0.
\end{aligned} \tag{3.2}$$

Definition 3.1. (ρ^n, u^n, v^n) are said to be well-prepared data if they satisfy,

$$\rho^n = \left(1 - \frac{\gamma-1}{\gamma A}\phi\right)^{\frac{1}{\gamma-1}} + O(\varepsilon^2) = \rho_0 + \varepsilon^2\rho^{(2)n} + \mathcal{O}(\varepsilon^3), \qquad \nabla\cdot(\rho_0\mathbf{u}^{(0)n}) = 0. \tag{3.3}$$

Lemma 3.2. *Choose (ρ^n, u^n, v^n) to be well-prepared and let a_0 as in (2.5), then when $\varepsilon \ll 1$,*

$$\mathcal{L} = \frac{1}{\varepsilon^2}\rho^n\left[\nabla N(\rho^n) + \nabla\phi - a^n[\nabla M(\rho^n) - \nabla\ln\rho_0]\right] = \rho_0\nabla\left[(N(\rho^n))^{(2)} - a_0(M(\rho^n))^{(2)}\right] + O(\varepsilon).$$

Proof. Let the expansion of a^n be given by

$$a^n = a^{(0)n} + \varepsilon a^{(1)n} + \varepsilon^2 a^{(2)n} + \mathcal{O}(\varepsilon^3). \tag{3.4}$$

Due to (3.3), from the definition $a(t) = (1-\varepsilon^2)\min_x\left\{p'(\rho)\right\}$, we find

$$a^{(0)n} = \min_x\left\{p'(\rho_0)\right\} = a_0, \qquad a^{(1)n} = 0. \tag{3.5}$$

Moreover, the expansions of $M(\rho^n) = M^n$ and $N(\rho^n) = N^n$ around $\rho^{(0)}$ are given as

$$\begin{aligned} M^n = M(\rho^n) =& M\big(\rho_0 + \varepsilon^2\rho^{(2)n} + \mathcal{O}(\varepsilon^3)\big), \\ =& M(\rho_0) + \varepsilon^2\rho^{(2)n}M'(\rho_0) + \mathcal{O}(\varepsilon^3), \\ N^n = N(\rho^n) =& N(\rho_0) + \varepsilon^2\rho^{(2)n}N'(\rho_0) + \mathcal{O}(\varepsilon^3). \end{aligned} \tag{3.6}$$

Due to the definition of ρ_0, we have

$$\ln(\rho_0)^{\gamma-1} = \ln\big(1 - \frac{\gamma-1}{\gamma A}\phi\big),$$

Thus,

$$(\gamma-1)\frac{\nabla\rho_0}{\rho_0} = \frac{-\frac{\gamma-1}{\gamma A}\nabla\phi}{(1-\frac{\gamma-1}{\gamma A}\phi)},$$

which gives

$$(\nabla M^n)^{(0)} - \nabla\ln\rho_0 = \nabla M(\rho_0) - \nabla\ln\rho_0 = 0.$$

Similarly, using the definitions of $N(\rho)$ in (3.1), we have

$$(\nabla N^n)^{(0)} + \nabla\phi = \nabla N(\rho_0) + \nabla\phi = 0.$$

Therefore, from the above results, we find

$$\begin{aligned} \mathcal{L} =& \frac{\rho_0}{\varepsilon^2}\left[(\nabla N^n)^{(0)} + \nabla\phi - a^{(0)n}\big[(\nabla M^n)^{(0)} - \nabla\ln\rho_0\big]\right] \\ &+ \frac{\rho_0}{\varepsilon}\left[(\nabla N^n)^{(1)} - a^{(0)n}(\nabla M^n)^{(1)} - a^{(1)n}\big[(\nabla M^n)^{(0)} - \nabla\ln\rho_0\big]\right] \\ &+ \rho_0\left[(\nabla N^n)^{(2)} - a^{(0)n}(\nabla M^n)^{(2)} - a^{(1)n}(\nabla M^n)^{(1)} - a^{(2)n}[(\nabla M^n)^{(0)} - \nabla\ln\rho_0]\right] \\ &+ \rho^{(2)n}\left[(\nabla N^n)^{(0)} + \nabla\phi - a^{(0)n}\big[(\nabla M^n)^{(0)} - \nabla\ln\rho_0\big]\right] + \mathcal{O}(\varepsilon) \\ =& \rho^{(0)}\big[(\nabla N^n)^{(2)} - a^{(0)n}(\nabla M^n)^{(2)}\big] + \mathcal{O}(\varepsilon) \\ =& \rho^{(0)}\nabla\big((N^n)^{(2)} - a_0(M^n)^{(2)}\big) + \mathcal{O}(\varepsilon). \end{aligned}$$

Hence, we conclude the proof of the lemma. ∎

Then we compare $\mathcal{O}(\frac{1}{\varepsilon^2})$ terms in the momentum equation (3.2) and the only terms left of order $\frac{1}{\varepsilon^2}$ are

$$a^{(0)n}\rho^{(0)n+1}\big[(\nabla M^{n+1})^{(0)} - \nabla\ln\rho_0\big] = 0.$$

Since $a^{(0)n} = a_0 \neq 0$, when $\rho^{(0)n+1} \neq 0$,

$$(\nabla M^{n+1})^{(0)} = \nabla \ln \rho_0, \tag{3.7}$$

which yields

$$\nabla \ln(\rho^{(0)n+1}) = \nabla \ln(1 - \frac{\gamma - 1}{\gamma A}\phi)^{\frac{1}{\gamma-1}}.$$

Thus

$$\ln(\rho^{(0)n+1})^{\gamma-1} = \ln(1 - \frac{\gamma - 1}{\gamma A}\phi) + c,$$

and $\rho^{(0)n+1}$ satisfies

$$\rho^{(0)n+1} = c\left(1 - \frac{\gamma - 1}{\gamma A}\phi\right)^{\frac{1}{\gamma-1}}.$$

Here c is an arbitrary constant determined by the boundary condition of ρ. If the boundary condition of ρ does not change with time, from the definition of $\phi(x)$, we find $\rho^{(0)n+1} = \rho_0$. The $\mathcal{O}(\frac{1}{\varepsilon})$ terms in the momentum equation (3.2) are

$$a^{(0)n}\rho^{(0)n+1}(\nabla M^{n+1})^{(1)} + \big(a^{(0)n}\rho^{(1)n+1} + a^{(1)n}\rho^{(0)n+1}\big)\nabla\big[M^{(0)n+1} - \ln \rho_0\big] = 0,$$

Due to (3.7), $(\nabla M^{n+1})^{(1)} = 0$. The boundary condition of ρ^{n+1} leads to $\rho^{(1)n+1} = 0$.

Now compare $\mathcal{O}(1)$ terms in the density equation in (2.8),

$$\frac{\rho^{(0)n+1} - \rho^{(0)n}}{\Delta t} + \alpha\nabla \cdot (\rho^{(0)}\mathbf{u}^{(0)})^n + (1 - \alpha)\nabla \cdot (\rho^{(0)}\mathbf{u}^{(0)})^{n+1} = 0, \tag{3.8}$$

Because $\rho^{(0)n+1} = \rho^{(0)n} = \rho_0$ is time independent and the initial data are well prepared, then equation (3.8) gives

$$\nabla \cdot (\rho_0\mathbf{u}^{(0)n+1}) = 0. \tag{3.9}$$

Compare $\mathcal{O}(1)$ terms in the momentum equation,

$$\begin{aligned}
&\frac{(\rho^{(0)}\mathbf{u}^{(0)})^{n+1} - (\rho^{(0)}\mathbf{u}^{(0)})^n}{\Delta t} + \nabla \cdot (\rho^{(0)}\mathbf{u}^{(0)} \otimes \mathbf{u}^{(0)})^n + \rho^{(0)n}\nabla\big((N^n)^{(2)} - a^{(0)n}(M^n)^{(2)}\big) \\
&+ a^{(0)n}\rho^{(0)n+1}(\nabla M^{n+1})^{(2)} + \big(a^{(0)n}\rho^{(1)n+1} + a^{(1),n}\rho^{(0)n+1}\big)(\nabla M^{n+1})^{(1)} \\
&+ \Big(a^{(0)n}\rho^{(2)n+1} + a^{(1)n}\rho^{(1)n+1} + a^{(2)n}\rho^{(0)n+1}\Big)\nabla\big[M^{(0)n+1} - \ln \rho_0\big] = 0.
\end{aligned}$$

Using the fact that $\rho^{(0)n+1} = \rho^{(0)n} = \rho_0$ is constant in time, $(\nabla M^{n+1})^{(0)} = \nabla \ln \rho_0$, and $(\nabla M^{n+1})^{(1)} = 0$, the equation simplifies to,

$$\frac{\mathbf{u}^{(0)n+1} - \mathbf{u}^{(0)n}}{\Delta t} + \mathbf{u}^{(0)n}\nabla \cdot \mathbf{u}^{(0)n} + \nabla(N^n - a_0M^n + a_0M^{n+1})^{(2)} = 0.$$

Therefore, as ε goes to zero, the solution of (2.8) converges to

$$\begin{aligned}
&\nabla \cdot (\rho^{(0)}\mathbf{u}^{(0)})^{n+1} = 0, \\
&\frac{\mathbf{u}^{(0)n+1} - \mathbf{u}^{(0)n}}{\Delta t} + \mathbf{u}^{(0)n}\nabla \cdot \mathbf{u}^{(0)n} + (\nabla W^{n+1})^{(2)} \quad = 0,
\end{aligned} \tag{3.10}$$

with $W^{n+1} = N^n - a_0M^n + a_0M^{n+1}$. Therefore, (3.10) is a good discretization of the incompressible limit equations (1.7) and the semi-discrete scheme (2.8) is AP.

3.2. **The AP property of the fully-discretized scheme**

As we did at the PDE level, we take the gravitational terms in the momentum equations in system (3.11) to the left-hand side and reformulate the system as follows:

$$\begin{cases}
\frac{\rho^{n+1}_{i+\frac12,j+\frac12}-\rho^{n}_{i+\frac12,j+\frac12}}{\Delta t}+\alpha\left[\frac{(F^n)^{Up,x}_{i+1,j+\frac12}-(F^n)^{Up,x}_{i,j+\frac12}}{\Delta x}+\frac{(F^n)^{Up,y}_{i+\frac12,j+1}-(F^n)^{Up,y}_{i+\frac12,j}}{\Delta y}\right]\\
+(1-\alpha)\left[\frac{(F^{n+1})^{Up,x}_{i+1,j+\frac12}-(F^{n+1})^{Up,x}_{i,j+\frac12}}{\Delta x}+\frac{(F^{n+1})^{Up,y}_{i+\frac12,j+1}-(F^{n+1})^{Up,y}_{i+\frac12,j}}{\Delta y}\right]=0,\\[2ex]
\frac{\rho^{n+1}_{i,j+\frac12}u^{n+1}_{i,j+\frac12}-\rho^{n}_{i,j+\frac12}u^{n}_{i,j+\frac12}}{\Delta t}+\frac{\zeta^{u,x}_{i+\frac12,j+\frac12}-\zeta^{u,x}_{i-\frac12,j+\frac12}}{\Delta x}+\frac{\zeta^{u,y}_{i,j+1}-\zeta^{u,y}_{i,j}}{\Delta y}\\
+\frac{1}{\varepsilon^2}\rho^n_{i,j+\frac12}\Big[D^x_{i,j+\frac12}N^n+D^x_{i,j+\frac12}\phi-a^n[D^x_{i,j+\frac12}M^n-D^x_{i,j+\frac12}\ln\rho_0]\Big]\\
+\frac{a^n}{\varepsilon^2}\rho^{n+1}_{i,j+\frac12}[D^x_{i,j+\frac12}M^{n+1}-D^x_{i,j+\frac12}\ln\rho_0]=0,\\[2ex]
\frac{\rho^{n+1}_{i+\frac12,j}v^{n+1}_{i+\frac12,j}-\rho^{n}_{i+\frac12,j}v^{n}_{i+\frac12,j}}{\Delta t}+\frac{\zeta^{v,x}_{i+1,j}-\zeta^{v,x}_{i,j}}{\Delta x}+\frac{\zeta^{v,y}_{i+\frac12,j+\frac12}-\zeta^{v,y}_{i+\frac12,j-\frac12}}{\Delta y}\\
+\frac{1}{\varepsilon^2}\rho^n_{i+\frac12,j}\Big[D^y_{i+\frac12,j}N^n+D^y_{i+\frac12,j}\phi-a^n[D^y_{i+\frac12,j}M^n-D^y_{i+\frac12,j}\ln\rho_0]\Big]\\
+\frac{a^n}{\varepsilon^2}\rho^{n+1}_{i+\frac12,j}[D^y_{i+\frac12,j}M^{n+1}-D^y_{i+\frac12,j}\ln\rho_0]=0.
\end{cases}\tag{3.11}$$

with

$$D^x_{i,j+\frac12}q=\frac{q_{i+\frac12,j+\frac12}-q_{i-\frac12,j+\frac12}}{\Delta x},\qquad D^y_{i+\frac12,j}q=\frac{q_{i+\frac12,j+\frac12}-q_{i+\frac12,j-\frac12}}{\Delta y}$$

for arbitrary function q We will show the AP property based on (3.11).

Assume that the Chapman-Enskog asymptotic expansion of the discrete variables are

$$\begin{aligned}
\rho^n_{i+\frac12,j+\frac12}&=\rho^{(0)n}_{i+\frac12,j+\frac12}+\varepsilon\rho^{(1)n}_{i+\frac12,j+\frac12}+\varepsilon^2\rho^{(2)n}_{i+\frac12,j+\frac12}+...,\\
u^n_{i,j+\frac12}&=u^{(0)n}_{i,j+\frac12}+\varepsilon u^{(1)n}_{i,j+\frac12}+\varepsilon^2u^{(2)n}_{i,j+\frac12}+...,\\
v^n_{i+\frac12,j}&=v^{(0)n}_{i+\frac12,j}+\varepsilon v^{(1)n}_{i+\frac12,j}+\varepsilon^2v^{(2)n}_{i+\frac12,j}+....
\end{aligned}$$

Definition 3.3. The discrete data (ρ,u,v) are said to be well-prepared if they satisfy,

$$\begin{aligned}
&\rho^n_{i+\frac12,j+\frac12}=\left(1-\frac{\gamma-1}{\gamma A}\phi_{i+\frac12,j+\frac12}\right)^{\frac{1}{\gamma-1}}+O(\varepsilon^2)=\rho^{(0)}_{i+\frac12,j+\frac12}+O(\varepsilon^2)\\
&\frac{(F^{(0)n})^{Up,x}_{i+1,j+\frac12}-(F^{(0)n})^{Up,x}_{i,j+\frac12}}{\Delta x}+\frac{(F^{(0)n})^{Up,y}_{i+\frac12,j+1}-(F^{(0)n})^{Up,y}_{i+\frac12,j}}{\Delta y}=0,
\end{aligned}\tag{3.12}$$

where $(F^{(0)n})^{Up,x}$, $(F^{(0)n})^{Up,y}$ are defined as in (2.14) with ρ^{n+1}, u^{n+1}, v^{n+1} being replaced by $\rho^{(0)n}$, $u^{(0)n}$ and $v^{(0)n}$.

Lemma 3.4. *Choose (ρ^n,u^n,v^n) to be well-prepared, then*

$$\begin{aligned}
\mathcal{L}_d&=\frac{1}{\varepsilon^2}\rho^n_{i,j+\frac12}\Big[D^x_{i,j+\frac12}N^n+D^x_{i,j+\frac12}\phi-a^n[D^x_{i,j+\frac12}M^n-D^x_{i,j+\frac12}\ln\rho_0]\Big]\\
&=\rho^{(0)}_{i,j+\frac12}D^x_{i,j+\frac12}\Big[N^{n(2)}-a_0M^{n(2)}\Big]+O(\varepsilon).
\end{aligned}$$

Proof. It is easy to check that

$$
\begin{aligned}
&D^x_{i,j+\frac{1}{2}} M(\rho^{(0)}) - D^x_{i,j+\frac{1}{2}} \ln \rho_0 = 0, \qquad D^y_{i+\frac{1}{2},j} M(\rho^{(0)}) - D^y_{i+\frac{1}{2},j} \ln \rho_0 = 0, \\
&D^x_{i,j+\frac{1}{2}} N(\rho^{(0)}) = \frac{A\gamma}{\gamma-1} D^x_{i,j+\frac{1}{2}} (\rho^{(0)})^{\gamma-1} = -D^x_{i,j+\frac{1}{2}} \phi, \quad D^y_{i+\frac{1}{2},j} N(\rho^{(0)}) + D^y_{i+\frac{1}{2},j} \phi = 0, \\
&\left(D^x_{i,j+\frac{1}{2}} M^n\right)^{(1)} = \left(D^x_{i,j+\frac{1}{2}} N^n\right)^{(1)} = 0, \qquad \left(D^y_{i+\frac{1}{2},j} M^n\right)^{(1)} = \left(D^y_{i+\frac{1}{2},j} N^n\right)^{(1)} = 0.
\end{aligned} \tag{3.13}
$$

The expansion of a^n is the same as in (3.4), (3.5). Now, let's look at the expansion of $\mathcal{L}_d$. Noting $a^{(0)n} = a_0$ and (3.13), we have

$$
\begin{aligned}
\mathcal{L}_d =& \frac{1}{\varepsilon^2} \rho^{(0)}_{i,j+\frac{1}{2}} \left[(D^x_{i,j+\frac{1}{2}} N^n)^{(0)} + D^x_{i,j+\frac{1}{2}} \phi - a^{(0)n} [(D^x_{i,j+\frac{1}{2}} M^n)^{(0)} - D^x_{i,j+\frac{1}{2}} \ln \rho_0] \right] \\
&+ \rho^{(0)}_{i,j+\frac{1}{2}} \left[(D^x_{i,j+\frac{1}{2}} N^n)^{(2)} - a^{(0)n} (D^x_{i,j+\frac{1}{2}} M^n)^{(2)} - a^{(2)n} [(D^x_{i,j+\frac{1}{2}} M^n)^{(0)} - D^x_{i,j+\frac{1}{2}} \ln \rho_0] \right] \\
&+ \rho^{(2)n}_{i,j+\frac{1}{2}} \left[(D^x_{i,j+\frac{1}{2}} N^n)^{(0)} + D^x_{i,j+\frac{1}{2}} \phi - a^{(0)n} [(D^x_{i,j+\frac{1}{2}} M^n)^{(0)} - D^x_{i,j+\frac{1}{2}} \ln \rho_0] \right] + \mathcal{O}(\varepsilon), \\
=& \rho^{(0)n}_{i,j+\frac{1}{2}} D^x_{i,j+\frac{1}{2}} \left[(N^n)^{(2)} - a_0 (M^n)^{(2)} \right] + \mathcal{O}(\varepsilon),
\end{aligned}
$$

which conclude the proof. ∎

Similarly,

$$
\begin{aligned}
&\frac{1}{\varepsilon^2} \rho^n_{i+\frac{1}{2},j} \left[D^y_{i+\frac{1}{2},j} N^n + D^y_{i+\frac{1}{2},j} \phi - a^n_d [D^y_{i+\frac{1}{2},j} M^n - D^y_{i+\frac{1}{2},j} \ln \rho_0] \right] \\
=& \rho^{(0)n}_{i+\frac{1}{2},j} D^x_{i+\frac{1}{2},j} \left[(N^n)^{(2)} - a_0 (M^n)^{(2)} \right] + \mathcal{O}(\varepsilon).
\end{aligned}
$$

Comparing the $\mathcal{O}(\frac{1}{\varepsilon^2})$ terms in the momentum equation in the x-direction, one gets

$$
a_0 \rho^{(0)n+1}_{i,j+\frac{1}{2}} [(D^x_{i,j+\frac{1}{2}} M^{n+1})^{(0)} - D^x_{i,j+\frac{1}{2}} \ln \rho_0] = 0. \tag{3.14}
$$

Because $a_0 \neq 0$ and $\rho^{(0),n+1}_{i,j+\frac{1}{2}} \neq 0$, then

$$
D^x_{i,j+\frac{1}{2}} \ln \rho^{(0)n+1} = D^x_{i,j+\frac{1}{2}} \ln (1 - \frac{\gamma-1}{\gamma A} \phi)^{\frac{1}{\gamma-1}}.
$$

Hence, the boundary conditions of ρ^{n+1} yield

$$
\rho^{(0)n+1}_{i+\frac{1}{2},j+\frac{1}{2}} = \left(1 - \frac{\gamma-1}{\gamma A} \phi_{i+\frac{1}{2},j+\frac{1}{2}} \right)^{\frac{1}{\gamma-1}}
$$

Similar result can be obtained from comparing $\mathcal{O}(\frac{1}{\varepsilon^2})$ terms in the momentum equation in the y-direction. From the above calculations, we deduce that $\rho^{(0)}_{i+\frac{1}{2},j+\frac{1}{2}}$ is independent of time. Similarly, comparing $\mathcal{O}(\frac{1}{\varepsilon})$ terms in the momentum equation gives $\rho^{(1)}_{i+\frac{1}{2},j+\frac{1}{2}} = 0$. From $\mathcal{O}(1)$ terms in the density equation,

$$
\begin{aligned}
&\alpha \left[\frac{(F^{n(0)})^{Up,x}_{i+1,j+\frac{1}{2}} - (F^{n(0)})^{Up,x}_{i,j+\frac{1}{2}}}{\Delta x} + \frac{(F^{n(0)})^{Up,y}_{i+\frac{1}{2},j+1} - (F^{n(0)})^{Up,y}_{i+\frac{1}{2},j}}{\Delta y} \right] \\
&+ (1-\alpha) \left[\frac{(F^{n+1(0)})^{Up,x}_{i+1,j+\frac{1}{2}} - (F^{n+1(0)})^{Up,x}_{i,j+\frac{1}{2}}}{\Delta x} + \frac{(F^{n+1(0)})^{Up,y}_{i+\frac{1}{2},j+1} - (F^{n+1(0)})^{Up,y}_{i+\frac{1}{2},j}}{\Delta y} \right] = 0.
\end{aligned}
$$

Then since and $\rho^{(0)}_{i+\frac{1}{2},j+\frac{1}{2}}$ is time independent, from (2.14) and (3.12), one has

$$\frac{\big(\rho^{(0)}_{i+\frac{1}{2},j+\frac{1}{2}}\big[u^{n+1(0)}_{i+1,j+\frac{1}{2}}\big]^+ - \rho^{(0)}_{i+\frac{3}{2},j+\frac{1}{2}}\big[u^{n+1(0)}_{i+1,j+\frac{1}{2}}\big]^-\big) - \big(\rho^{(0)}_{i-\frac{1}{2},j+\frac{1}{2}}\big[u^{n+1(0)}_{i,j+\frac{1}{2}}\big]^+ - \rho^{(0)}_{i+\frac{1}{2},j+\frac{1}{2}}\big[u^{n+1(0)}_{i,j+\frac{1}{2}}\big]^-\big)}{\Delta x}$$
$$+\frac{\big(\rho^{(0)}_{i+\frac{1}{2},j+\frac{1}{2}}\big[v^{n+1(0)}_{i+\frac{1}{2},j+1}\big]^+ - \rho^{(0)}_{i+\frac{1}{2},j+\frac{3}{2}}\big[v^{n+1(0)}_{i+\frac{1}{2},j+1}\big]^-\big) - \big(\rho^{(0)}_{i+\frac{1}{2},j-\frac{1}{2}}\big[v^{n+1(0)}_{i+\frac{1}{2},j}\big]^+ - \rho^{(0)}_{i+\frac{1}{2},j+\frac{1}{2}}\big[v^{n+1(0)}_{i+\frac{1}{2},j}\big]^-\big)}{\Delta y} = 0. \tag{3.15}$$

Comparing $\mathcal{O}(1)$ terms in the momentum equation in x-direction and using (3.14), the equation can be simplified to,

$$\frac{u^{n+1(0)}_{i,j+\frac{1}{2}} - u^{n(0)}_{i,j+\frac{1}{2}}}{\Delta t} + \frac{1}{\rho^{(0)}_{i,j+\frac{1}{2}}}\frac{\zeta^{u,x}_{i+\frac{1}{2},j+\frac{1}{2}} - \zeta^{u,x}_{i-\frac{1}{2},j+\frac{1}{2}}}{\Delta x} + \frac{1}{\rho^{(0)}_{i,j+\frac{1}{2}}}\frac{\zeta^{u,y}_{i,j+1} - \zeta^{u,y}_{i,j}}{\Delta y}$$
$$+ D^x_{i,j+\frac{1}{2}}\big[(N^n)^{(2)} - a_0(M^n)^{(2)} + a_0(M^{n+1})^{(2)}\big] = 0.$$

Finally the momentum limit equation in the x-direction is,

$$\frac{u^{n+1(0)}_{i,j+\frac{1}{2}} - u^{n(0)}_{i,j+\frac{1}{2}}}{\Delta t} + \frac{1}{\rho^{(0)}_{i,j+\frac{1}{2}}}\frac{\zeta^{u,x}_{i+\frac{1}{2},j+\frac{1}{2}} - \zeta^{u,x}_{i-\frac{1}{2},j+\frac{1}{2}}}{\Delta x} + \frac{1}{\rho^{(0)}_{i,j+\frac{1}{2}}}\frac{\zeta^{u,y}_{i,j+1} - \zeta^{u,y}_{i,j}}{\Delta y} + \frac{W^{(2)n+1}_{i+\frac{1}{2},j+\frac{1}{2}} - W^{(2)n+1}_{i-\frac{1}{2},j+\frac{1}{2}}}{\Delta x} = 0. \tag{3.16}$$

Similar calculations are performed on the momentum equation in the y-direction, which yields

$$\frac{v^{n+1(0)}_{i+\frac{1}{2},j} - v^{n(0)}_{i+\frac{1}{2},j}}{\Delta t} + \frac{1}{\rho^{(0)}_{i+\frac{1}{2},j}}\frac{\zeta^{v,x}_{i+1,j} - \zeta^{v,x}_{i,j}}{\Delta x} + \frac{1}{\rho^{(0)}_{i+\frac{1}{2},j}}\frac{\zeta^{v,y}_{i+\frac{1}{2},j+\frac{1}{2}} - \zeta^{u,y}_{i+\frac{1}{2},j-\frac{1}{2}}}{\Delta y} + \frac{W^{(2)n+1}_{i+\frac{1}{2},j+\frac{1}{2}} - W^{(2)n+1}_{i+\frac{1}{2},j-\frac{1}{2}}}{\Delta y} = 0. \tag{3.17}$$

Therefore, the fully-discrete incompressible limit system is (3.15)-(3.17). It is not difficult to check that (3.15)-(3.17) is a consist discretization of the incompressible limit system (1.7).

3.3. **The WB property of the scheme**

In this section we prove that the developed AP scheme for the isentropic Euler equations with gravitational source term is WB. The stationary state under consideration is

$$u^s_{i,j+\frac{1}{2}} = v^s_{i+\frac{1}{2},j} = 0, \qquad \rho^s_{i+\frac{1}{2},j+\frac{1}{2}} = \Big(1 - \frac{\gamma-1}{\gamma A}\phi_{i+\frac{1}{2},j+\frac{1}{2}}\Big)^{\frac{1}{\gamma-1}}.$$

Theorem 3.5. *If the solution at time t^n is stationary, i.e. $(\rho^n_{i+\frac{1}{2},j+\frac{1}{2}}, u^n_{i,j+\frac{1}{2}}, v^n_{i+\frac{1}{2},j}) = (\rho^s_{i+\frac{1}{2},j+\frac{1}{2}}, u^s_{i,j+\frac{1}{2}}, v^s_{i+\frac{1}{2},j})$, then it does not change at the next time t^{n+1}.*

Proof. By substituting $(\rho^n_{i+\frac{1}{2},j+\frac{1}{2}}, u^n_{i,j+\frac{1}{2}}, v^n_{i+\frac{1}{2},j}) = (\rho^s_{i+\frac{1}{2},j+\frac{1}{2}}, u^s_{i,j+\frac{1}{2}}, v^s_{i+\frac{1}{2},j})$ into (3.11), it is easy to check that

$$D^x_{i,j+\frac{1}{2}}N^n + D^x_{i,j+\frac{1}{2}}\phi = 0, \qquad D^y_{i+\frac{1}{2},j}N^n + D^y_{i+\frac{1}{2},j}\phi = 0,$$
$$D^x_{i,j+\frac{1}{2}}M^n - D^x_{i,j+\frac{1}{2}}\ln\rho_0 = 0, \qquad D^y_{i+\frac{1}{2},j}M^n - D^y_{i+\frac{1}{2},j}\ln\rho_0 = 0,$$

and for $\forall\varepsilon$, (3.11) becomes

$$\begin{cases} \frac{\rho^{n+1}_{i+\frac{1}{2},j+\frac{1}{2}}-\rho^{n}_{i+\frac{1}{2},j+\frac{1}{2}}}{\Delta t}+(1-\alpha)\left[\frac{(F^{n+1})^{Up,x}_{i+1,j+\frac{1}{2}}-(F^{n+1})^{Up,x}_{i,j+\frac{1}{2}}}{\Delta x}+\frac{(F^{n+1})^{Up,y}_{i+\frac{1}{2},j+1}-(F^{n+1})^{Up,y}_{i+\frac{1}{2},j}}{\Delta y}\right]=0, \\ \frac{\rho^{n+1}_{i,j+\frac{1}{2}}u^{n+1}_{i,j+\frac{1}{2}}}{\Delta t}+\frac{a^n}{\varepsilon^2}\rho^{n+1}_{i,j+\frac{1}{2}}[D^x_{i,j+\frac{1}{2}}M^{n+1}-D^x_{i,j+\frac{1}{2}}\ln\rho_0]=0, \\ \frac{\rho^{n+1}_{i+\frac{1}{2},j}v^{n+1}_{i+\frac{1}{2},j}}{\Delta t}+\frac{a^n}{\varepsilon^2}\rho^{n+1}_{i+\frac{1}{2},j}[D^y_{i+\frac{1}{2},j}M^{n+1}-D^y_{i+\frac{1}{2},j}\ln\rho_0]=0. \end{cases} \tag{3.18}$$

One can check that $(\rho^{n+1}_{i+\frac{1}{2},j+\frac{1}{2}}, u^{n+1}_{i,j+\frac{1}{2}}, v^{n+1}_{i+\frac{1}{2},j}) = (\rho^{s}_{i+\frac{1}{2},j+\frac{1}{2}}, u^{s}_{i,j+\frac{1}{2}}, v^{s}_{i+\frac{1}{2},j})$ satisfies (3.18), this concludes the proof of the WB property of the fully-discretized scheme. ∎

4. Numerical Results

In this section, we validate the AP and WB properties of the 1D and 2D numerical schemes. Test cases are chosen for the isentropic Euler equations with and without gravitational source term. Note that, in the absence of the gravitational source term, the developed scheme is the AP scheme developed by Goudon et al. [11]. As in [11], we choose $\alpha = \varepsilon^2$ and $l = 0$ in the definition of $a(t)$ in (2.5)for all numerical test cases.

4.1. 1D test cases

4.1.1. *1D Riemann problem*

In order to validate the robustness of the 1D numerical scheme, we extract from [11] a 1D Riemann problem for different values of ε. The initial conditions are

$$\rho(x,0) = \begin{cases} 1+\varepsilon^2 & \text{if } x < 0.5, \\ 1 & \text{if } x > 0.5, \end{cases}$$

$$u(x,0) = \begin{cases} 1-\varepsilon & \text{if } x < 0.5, \\ 1+\varepsilon & \text{if } x > 0.5. \end{cases}$$

The pressure is given by $p(\rho) = A\rho^\gamma$ with $A = 1$ and $\gamma = 2$. The solution is computed in the interval $[0, 1]$ over 200 grid points for $\Delta t = \beta\Delta x$, with $\beta = 0.2, 0.1$ or 0.01. To test the AP property of the scheme, three different cases for different values of ε are considered. The density and the velocity are illustrated at the final time $T = 0.1$ for $\varepsilon = \sqrt{0.99}$ and $\beta = 0.2$ in figure 2, at the final time $T = 0.05$ for $\varepsilon = \sqrt{0.1}$ and $\beta = 0.1$ in figure 3, and at the final time $T = 0.007$ for $\varepsilon = \sqrt{0.001}$ and $\beta = 0.01$ in figure 4. In the cases where ε is small ($\varepsilon = \sqrt{0.1}$ or $\sqrt{0.001}$), the AP scheme gives relevant results for $\beta = 0.2$, while explicit scheme simply returns negative density. By adjusting β, the AP scheme gives better results, and the explicit scheme returns positive density. For more details about the comparison, please refer to section 3.1 in [11]. The plots are in prefect match with the ones in the Literature. The solution can still be captured as ε gets smaller which proves the AP property of the 1D scheme.

4.1.2. *1D steady state*

As proven analytically, the AP scheme is also WB. To prove numerically the WB property of the scheme, we simulate a steady state solution and prove numerically that the scheme preserves the

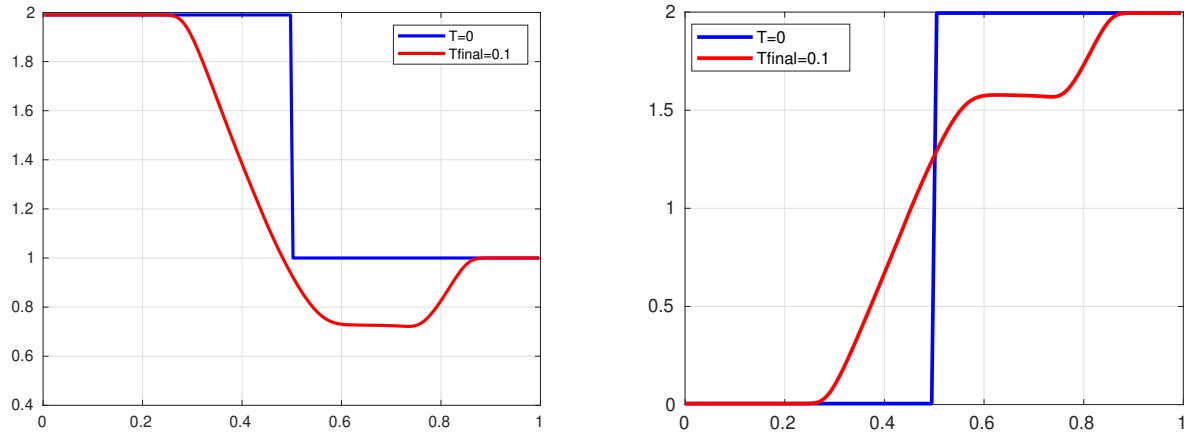

FIGURE 2. 1D Riemann problem: density (left) and velocity (right) initially and at the final time Tfinal=0.1 for $\varepsilon = \sqrt{0.99}$ and $\beta = 0.2$.

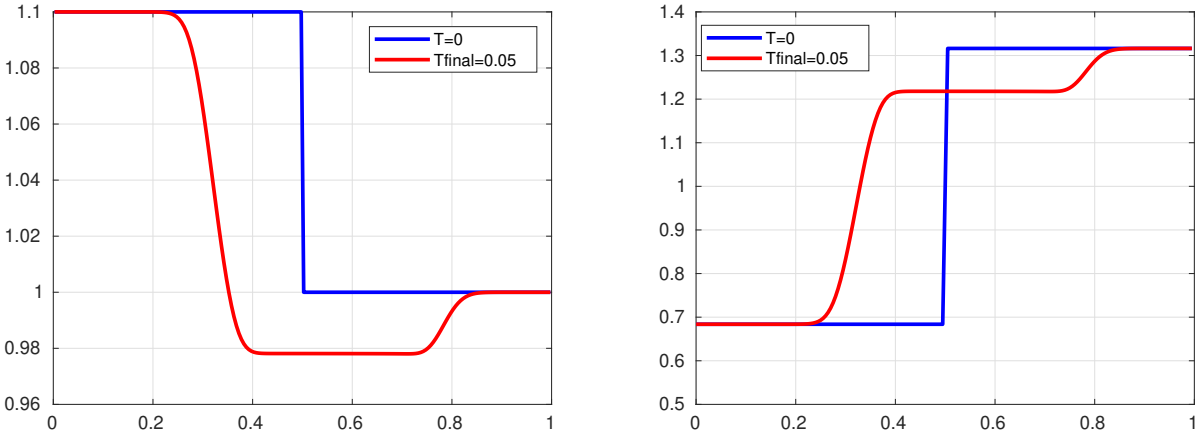

FIGURE 3. 1D Riemann problem: density (left) and velocity (right) initially and at the final time Tfinal=0.05 for $\varepsilon = \sqrt{0.1}$ and $\beta = 0.1$.

steady state. One example of a steady state for the isentropic Euler equations with gravitational source term is

$$\begin{cases} \rho(x) = \left(1 - \frac{\gamma-1}{\gamma A}\phi(x)\right)^{\frac{1}{\gamma-1}}, \\ u(x) = 0. \end{cases} \tag{4.1}$$

With the pressure law given as $p(\rho) = A\rho^\gamma$ where $A = 1$ and $\gamma = 1.4$, and a gravitational potential $\phi(x) = x$. At the PDE level, (4.1) is a steady state solution. The computational domain is the interval $[0, 1]$ discretized over 200 grid points. We choose $\varepsilon = \sqrt{0.99}$ and $\Delta t = \beta \Delta x$ with $\beta = 0.01$ With the knowledge that the scheme should preserve the steady state independent of the choice of ε. We run our simulations till the final time $t = 0.1$ and compare it to the steady state solution in figure 5. The density plot at the final time lies exactly on top of the initial density. The velocity error is approximately 10^{-7} and this error stays as it is as time increases, an indication that the scheme has

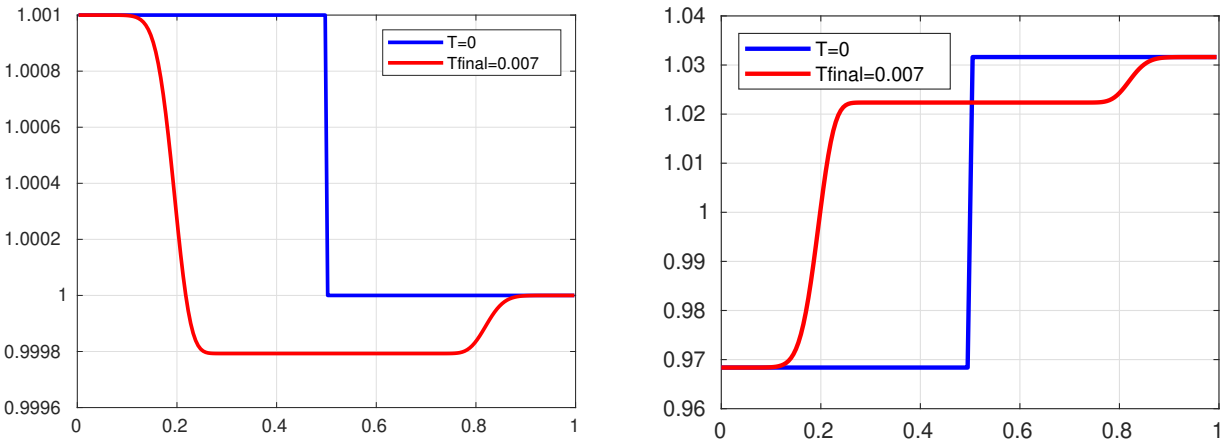

FIGURE 4. 1D Riemann problem: density (left) and velocity (right) initially and at the final time Tfinal=0.007 for $\varepsilon = \sqrt{0.001}$ and $\beta = 0.01$.

reached the numerical steady state. It is worth mentioning that no well-balancing treatment is applied here. In other words, the AP schemes with their IMEX structure fulfill the need for any SP treatment. At least for the isentropic Euler equations with gravitational source term, the SP property follows from the AP property.

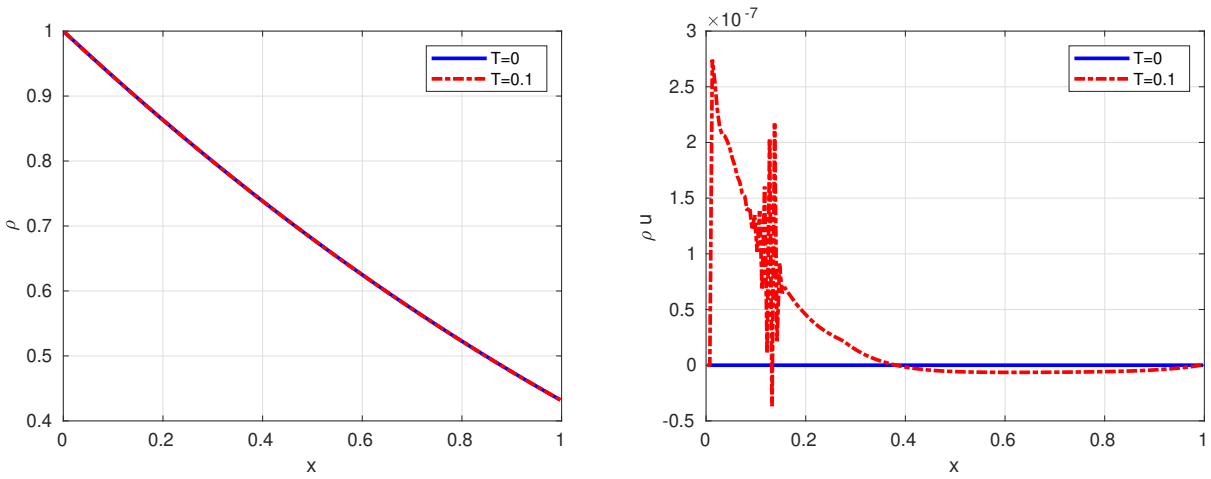

FIGURE 5. 1D steady state: profile of the density (left) and the momentum (right) initially and at the final time $t = 0.1$.

4.2. **2D test cases**

4.2.1. *2D Riemann problem*

An extension of the 1D Riemann Problem is considered in this section. The initial data are given as

$$\rho(x,y,0) = \begin{cases} 1+\varepsilon^2 & \text{if} \quad x < 0.5, \\ 1 & \text{if} \quad x > 0.5, \end{cases}$$

$$u(x,y,0) = \begin{cases} 1-\varepsilon & \text{if} \quad x < 0.5, \\ 1+\varepsilon & \text{if} \quad x > 0.5, \end{cases}$$

$$v(x,y,0) = 0.$$

The 1D flow in 2D setup takes place in the direction of the horizontal velocity. The computational domain is the square $(0,1)\times(0,1)$ divided into 200×200 grid points. A comparison between the 1D results and the 2D cross sections is illustrated. The density and the velocity are plotted at the final time $T = 0.1$ for $\varepsilon = \sqrt{0.99}$ and $\beta = 0.2$ in figure 6, at the final time $T = 0.05$ for $\varepsilon = \sqrt{0.1}$ and $\beta = 0.1$ in figure 7, and at the final time $T = 0.007$ for $\varepsilon = \sqrt{0.001}$ and $\beta = 0.01$ in figure 8. The results show the accuracy and the robustness of the 2D scheme (2.9)-(2.13) as well as the AP property.

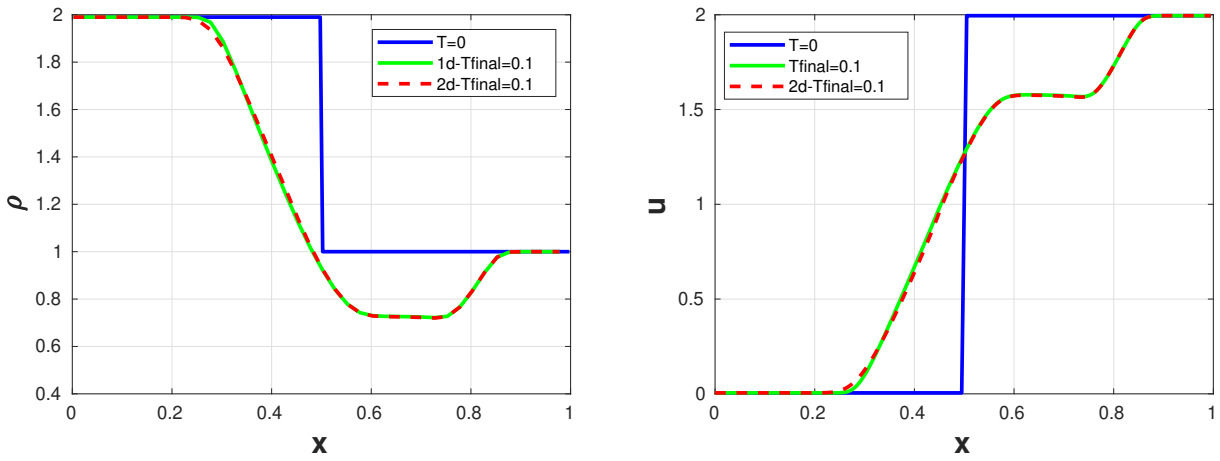

FIGURE 6. 2D Riemann problem: density (left) and velocity (right) initially, and at the final time Tfinal=0.1 for $\varepsilon = \sqrt{0.99}$ and $\beta = 0.2$.

4.2.2. *2D steady state*

In this section, we test the SP property of the 2D scheme. An extension of the 1D steady state along the y-axis is considered

$$\rho(x,y) = \left(1 - \frac{\gamma-1}{\gamma A}\phi(x,y)\right)^{\frac{1}{\gamma-1}}, \tag{4.2}$$

$$\tag{4.3}$$

with zero velocity field $\mathbf{u} = 0$ in the square $(0,1)\times(0,1)$ over 200×200 grid points, and a gravitational potential $\phi(x,y) = x$. A direct comparison between the 1D plots and the 2D cross sections is illustrated

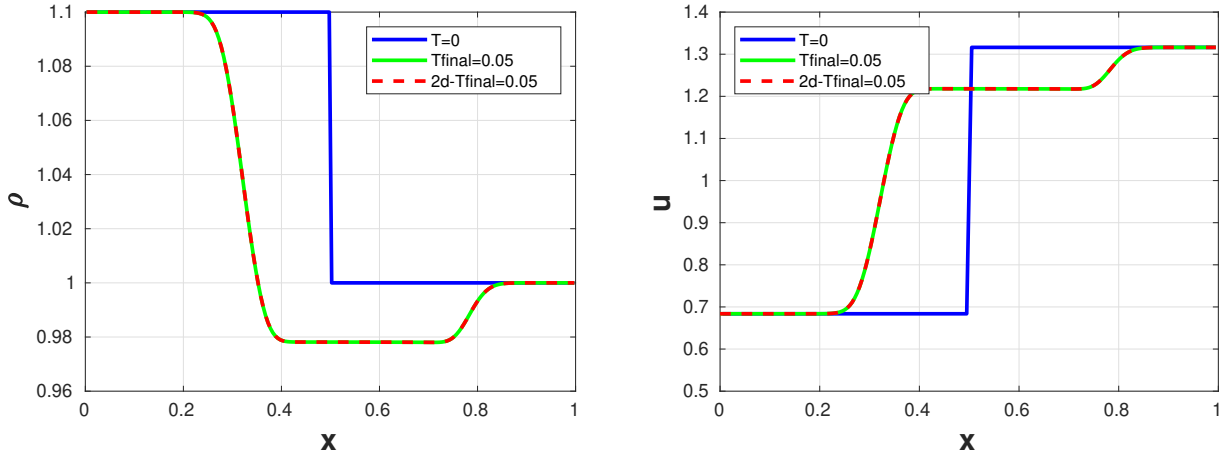

Figure 7. 2D Riemann problem: density (left) and velocity (right) initially, and at the final time Tfinal=0.05 for $\varepsilon = \sqrt{0.1}$ and $\beta = 0.1$.

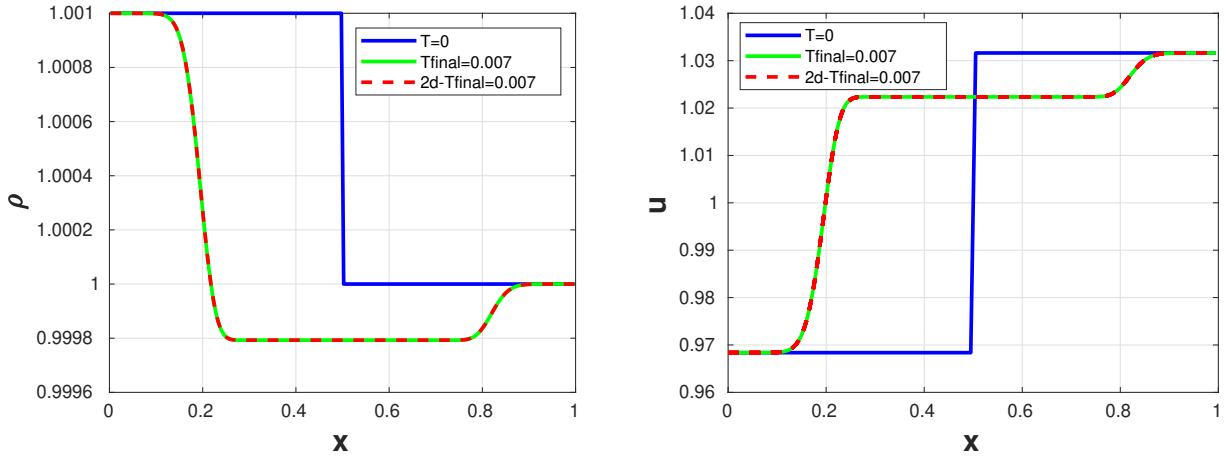

Figure 8. 2D Riemann problem: density (left) and velocity (right) initially, and at the final time Tfinal=0.007 for $\varepsilon = \sqrt{0.001}$ and $\beta = 0.01$.

in figure 9. This test case proves that the 2D AP scheme preserves steady states numerically without the need for any extra well-balancing, which is a strong statement, suggesting that we can prove, so far (analytically and numerically), for AP schemes for the isentropic Euler equations with gravitational source term.

4.2.3. *2D translating vortex*

A traveling vortex from [11] is considered in this section. The computational domain is the square $[0, 1] \times [0, 1]$ discretized over 32×32 grid points with $\varepsilon = 0.8$ and $\Delta t = 5 \times 10^{-4}$. The initial data are

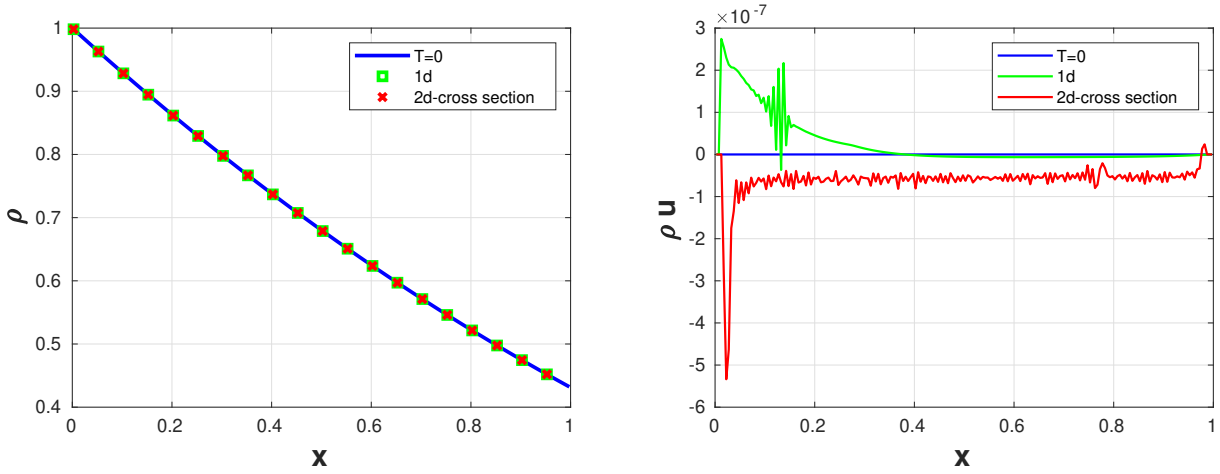

FIGURE 9. 2D steady state: profile of the density (left) and the momentum (right) initially and at the final time $t = 0.1$.

given as

$$\rho(x, y, 0) = 110 + \frac{\varepsilon^2}{(4\pi)^2} f(r), \tag{4.4}$$

$$u(x, y, 0) = \nu_0 + g(r)(0.5 - y), \tag{4.5}$$

$$v(x, y, 0) = \nu_1 + g(r)(x - 0.5), \tag{4.6}$$

$$\tag{4.7}$$

with

$$r = 4\pi((x - 0.5)^2 + (y - 0.5)^2))^{\frac{1}{2}},$$
$$f(r) = (1.5)^2 \Delta(r)(k(r) - k(\pi)),$$
$$g(r) = 1.5(1 + \cos(r))\Delta(r),$$
$$\Delta(r) = 1_{r<\pi}.$$

The pressure law is given as $p(\rho) = \frac{1}{2}\rho^2$ and $\nu_0 = 0.6, \nu_1 = 0$. We compare our computed numerical solution to the exact solution,

$$\rho(x, y, t) = \rho(x - \nu_0 t, y - \nu_1 t, 0), \tag{4.8}$$

$$u(x, y, 0) = u(x - \nu_0 t, y - \nu_1 t, 0), \tag{4.9}$$

$$v(x, y, 0) = v(x - \nu_0 t, y - \nu_1 t, 0). \tag{4.10}$$

$$\tag{4.11}$$

The vortex gets translated at speed (ν_0, ν_1), as one can see in figure 10. We present initially and at the final time, the horizontal velocity in figure 11, and the vertical velocity in figure 12. To avoid spurious oscillation, we set l in definition of $a(t)$ to 1.

4.2.4. *2D stationary vortex*

For our last test case, we consider a stationary vortex for the system of isentropic Euler equations with gravitational source term. The aim is to prove that our numerical scheme is both WB, as for a fixed ε, the vortex is a stationary solution of the system and AP, as the numerical solution becomes

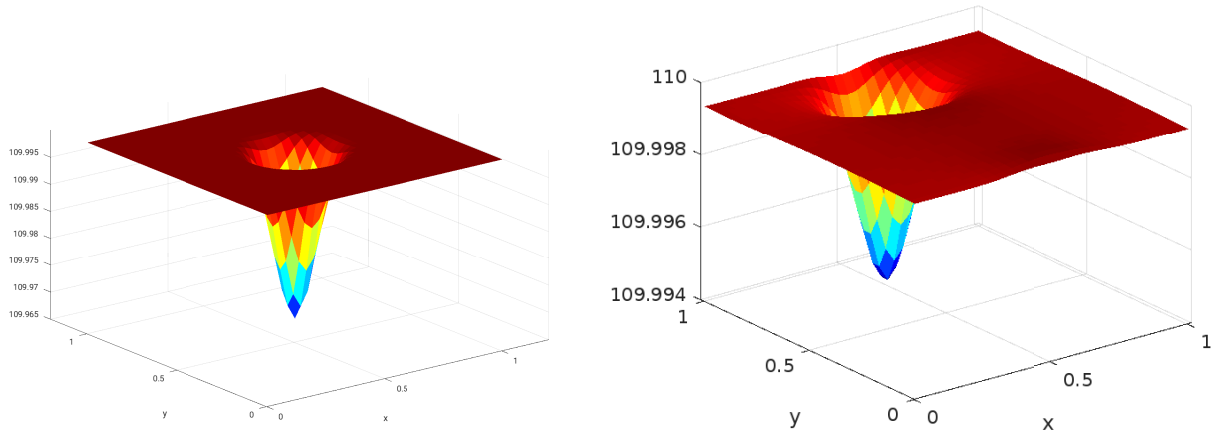

$\mathrm{T} = 0, \min_{i,j} \rho_{i+\frac{1}{2},j+\frac{1}{2}} = 109.9690$

$\mathrm{T} = 0.5, \min_{i,j} \rho_{i+\frac{1}{2},j+\frac{1}{2}} = 109.9951$

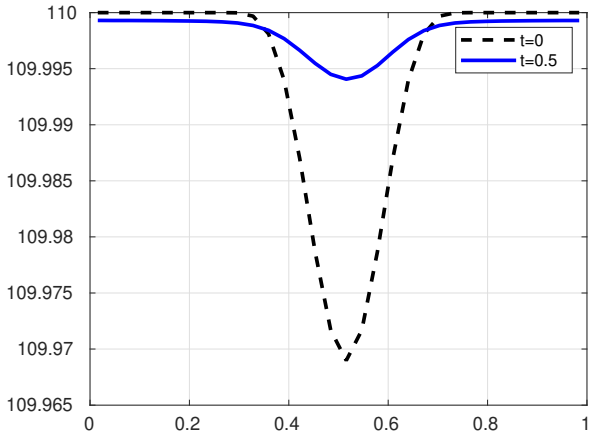

cut

FIGURE 10. Translating vortex: the initial (left) and final (middle) profile of the density ρ, and a cross section (right) along $y = 0.5$ as a function of $x - v_0 T$.

a solution of the incompressible version of the isentropic Euler system as ε goes to zero. We take the vortex for the shallow water equations defined in [18], and we change its initial data to fit the the rescaled shallow water equations. The initial condistions are given as,

$$\rho(x, y, t) = 1 - \phi(x, y), \qquad u(t, x, y) = ye^{1-r^2}, \qquad v(t, x, y) = -xe^{1-r^2}.$$

Here $r^2 = x^2 + y^2$, $\phi(x, y) = \frac{\varepsilon^2}{4} e^{2(1-r^2)} + 0.2e^{0.5(1-r^2)}$ is the gravitational potential. The pressure law is $p(\rho) = A\rho^\gamma$ with $A = \frac{1}{2}$ and $\gamma = 2$. The vortex rotates in the computational domain $(-1, 1)$ x $(-1, 1)$ with steady state boundary conditions over 32 x 32 grid points. Figure 13 illustrates the profile of the velocity $q = \sqrt{u^2 + v^2}$ initially and at the final time $t = 1$ for $\varepsilon = 10^{-1}, 10^{-2}, 10^{-3}, 10^{-4}$. The significance of this test case lies in the fact that the scheme preserves the steady state and at the same time converges as ε goes to zero. The result ensures the ability of our numerical scheme to preserve steady states and to capture the solution as ε gets smaller. This test case proves that the developed

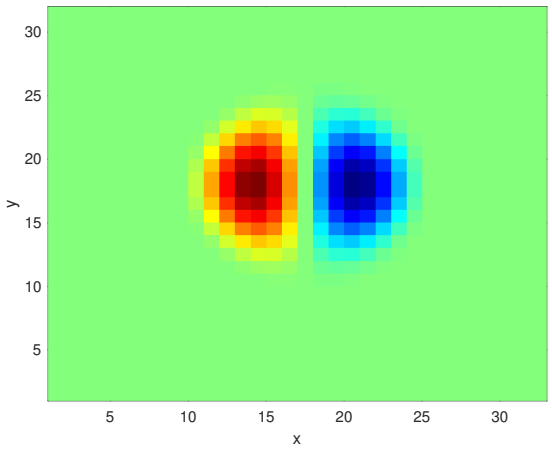

$\mathrm{T} = 0, \min_{i,j} u_{i,j+\frac{1}{2}} = 0.4098,$
$\max_{i,j} u_{i,j+\frac{1}{2}} = 0.7902.$

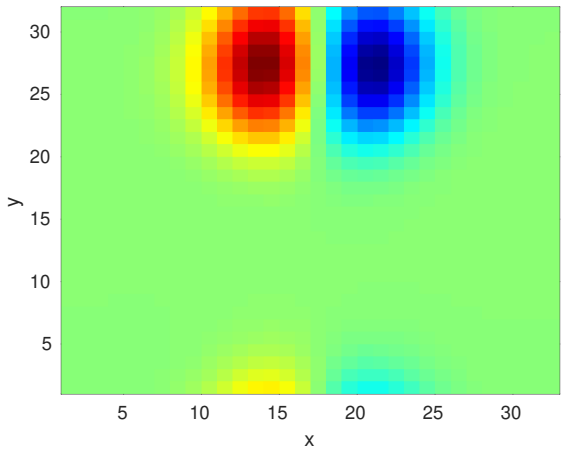

$\mathrm{T} = 0.5, \min_{i,j} u_{i,j+\frac{1}{2}} = 0.52,$
$\max_{i,j} u_{i,j+\frac{1}{2}} = 0.67.$

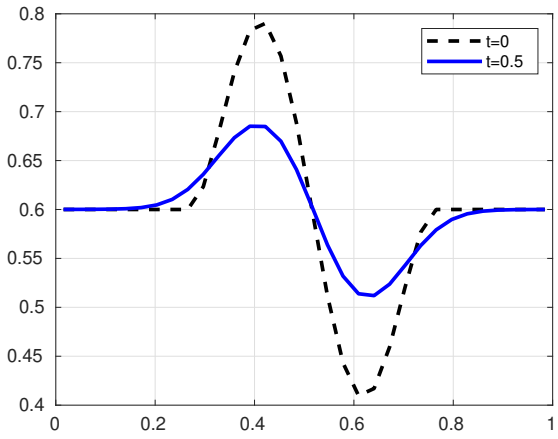

cut

FIGURE 11. Translating vortex: the initial (left) and final (middle) profile of the horizontal velocity u, and a cross section (right) along $x = 0.5 + v_0 T$ as a function of y.

numerical scheme for the system of isentropic Euler equations with gravitational source term is both AP and WB for all ε.

5. **Conclusion**

In this paper, an AP and WB scheme is proposed for the isentropic Euler equations with gravitational potential. The AP property is achieved by adding and subtracting certain terms that incorporate information about the spatially nonuniform density equilibrium. The WB property is achieved by introducing a special spatial discretization for both the source term and the pressure term, thereby balancing these two terms across all Mach numbers.

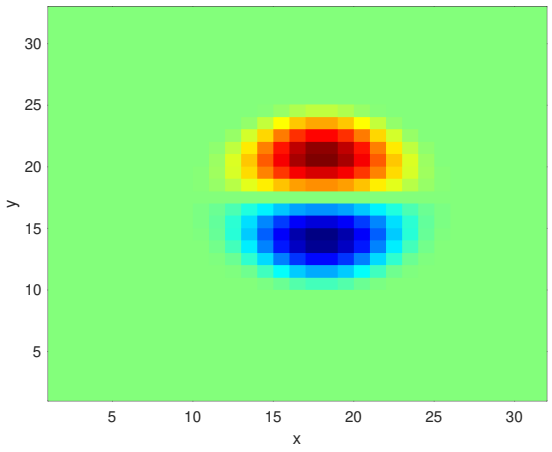

$\mathrm{T} = 0, \min_{i,j} v_{i+\frac{1}{2},j} = -0.1902,$
$\max_{i,j} v_{i+\frac{1}{2},j} = 0.1902.$

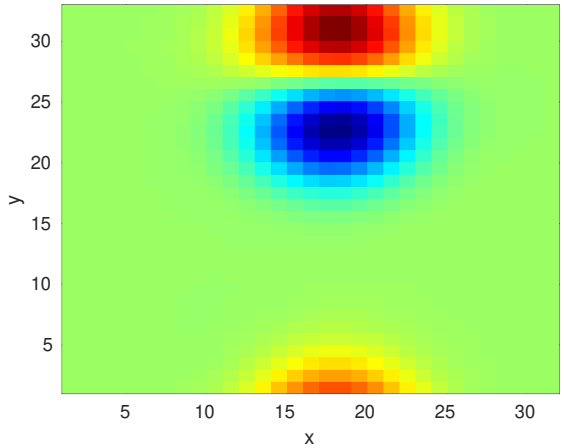

$\mathrm{T} = 0.5, \min_{i,j} v_{i+\frac{1}{2},j} = -0.069,$
$\max_{i,j} v_{i+\frac{1}{2},j} = 0.063.$

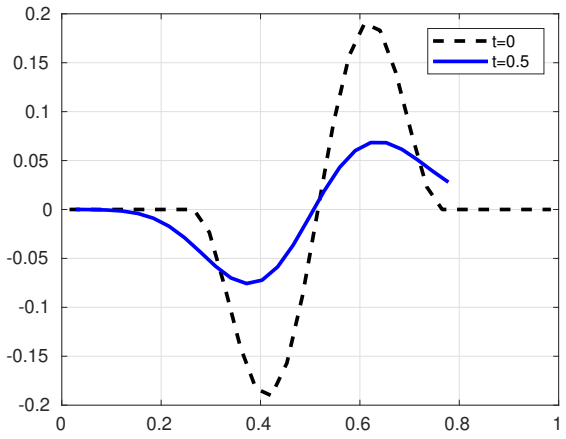

cut

FIGURE 12. Translating vortex: the initial (left) and final (middle) profile of the vertical velocity v, and a cross section (right) along $y = 0.5$ as a function of $x - v_0 T$.

The proof of the AP and WB properties at the semi-discrete level clearly depends on the pressure law and the fact that we are dealing with the isentropic case. Extending the current work to the full Euler equations with gravity is planned for future research.

Bibliography

[1] K. R. Arun and S. Samantaray. An asymptotic preserving time integrator for low mach number limits of the euler equations with gravity.

[2] S. Avgerinos, F. Bernard, A. Iollo, and Russo G. Linearly implicit all mach number shock capturing schemes for the euler equations. *Journal of Computational Physics*, 393:278–312, 2019.

[3] N. Botta, R. Klein, S. Langenberg, and S. Lützenkirchen. Well balanced finite volume methods for nearly hydrostatic flows. *Journal of Computational Physics*, 196:539–565, 2004.

[4] G. Bruell and Feireisl E. On a singular limit for stratified compressible fluids. *Nonlinear Analysis: Real World Applications*, 44(6):334–346, 2018.

[5] Alina Chertock, Shumo Cui, Alexander Kurganov, Şeyma Nur Özcan, and Eitan Tadmor. Well-balanced schemes for the euler equations with gravitation: Conservative formulation using global fluxes. *Journal of Computational Physics*, 358:36–52, 2018.

[6] F. Cordier, P. Degond, and A. Kumbaro. An asymptotic-preserving all-speed scheme for the euler and navier-stokes equations. *arXiv:1108.2876v1 [math-ph] 14 Aug 2011.*

[7] P. Degond and M. Tang. All speed scheme for the low mach number limit of the isentropic euler equations. *Commun. Comput. Phys.*, 10(1):1–31, 2011.

[8] G. Dimarco, R. Loubére, and M. Vignal. Study of a new asymptotic preserving scheme for the euler system in the low mach number limit. *SIAM J. SCI. COMPUT.*, 39(5):A2099–A2128, 2017.

[9] Feireisl E., C. Klingenberg, O. Kremla, and S. Markfelder. On oscillatory solutions to the complete euler system. *Journal of Differental Equations*, 269:1521–1543, 2020.

[10] F.G. Fuchs, A.D. McMurry, S. Mishra, N.H. Risebro, and K. Waagan. High order well-balanced finite volume schemes for simulating wave propagation in stratified magnetic atmospheres. *Journal of Computational Physics*, 229:4033–4058, 2010.

[11] T. Goudon, J. LIobell, and S. Minjeaud. An asymptotic preserving scheme on staggered grids for the barotropic euler system in low mach regimes. *Numer Methods Partial Differential Eq.*, pages 1–31, 2020.

[12] T. Goudon and S. Minjeaud. An explicit well-balanced scheme on staggered grids for the barotropic euler equations. *ESAIM: M2AN 58*, pages 1263–1299, 2024.

[13] Yaguang Gu, Zhen Gao, Guanghui Hu, Peng Li, and Qingcheng Fu. High order well-balanced positivity-preserving scale-invariant aweno scheme for euler systems with gravitational field. *Journal of Computational Physics*, 488:112190, 2023.

[14] J. Haack, S. Jin, and J.-G. Liu. An all-speed asymptotic preserving method for the isentropic euler and navier-stokes equations. *Numer Methods Partial Differential Eq.*, 2011.

[15] R. Hosek and B. She. Stability and consistency of a finite difference scheme for compressible viscous isentropic flow in multi-dimension. 2017.

[16] R. Klein. Semi-implicit extension of a godunov-type scheme based on low mach number asymptotics i" one-dimensional flow. *lnstitut für Technische Mechanik, RWTH*, 1995.

[17] R. Käppeli and S. Mishra. Well-balanced schemes for the euler equations with gravitation. *Journal of Computational Physics*, 259:199–219, 2014.

[18] V. Michel-Dansac, C. Berthon, S. Clain, and F. Foucher. A two-dimensional high-order well-balanced scheme for the shallow water equations with topography and manning friction. *hal-02536791*, 2020.

[19] F. Miczek, F.K. Röpke, and P.V.F Edelmann. New numerical solver for flows at various mach numbers. *A and A*, 576(A50):2182–2189, 2015.

[20] S. Noelle, G. Bispen, K. R. Arun, M. Lukácová-Medvidová, and C.-D. Munz. A weakly asymptotic preserving low mach number scheme for the euler equations of gas dynamics. *SIAM J. SCI. COMPUT.*, 36(6):B989–B1024, 2014.

[21] M. Tang. Second order all speed method for the isentropic euler equations. *Kinetic and Related Models*, 5(1):155–184, 2012.

[22] J. Zeifang, J. Schütz, K. Kaiser, Beck A., M. Lukácová-Medvidová, and S. Noelle. A novel full-euler low mach number imex splitting. *Global Science Preprint.*

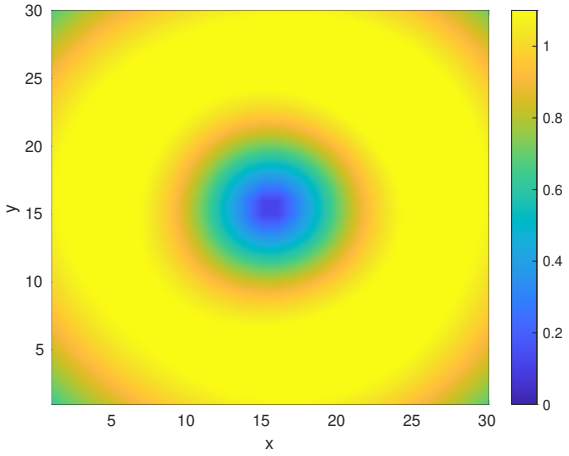

$T = 0$

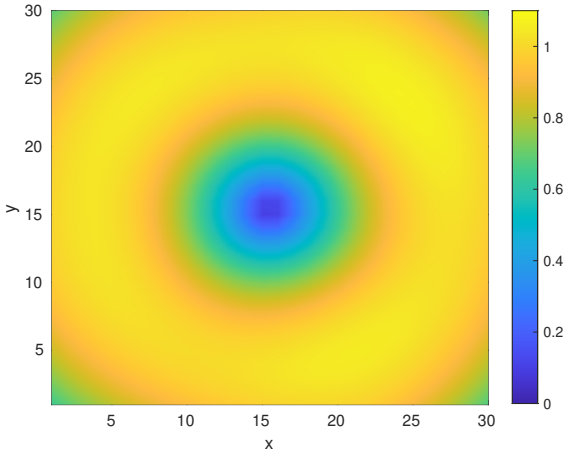

$T = 1, \varepsilon = 10^{-1}$

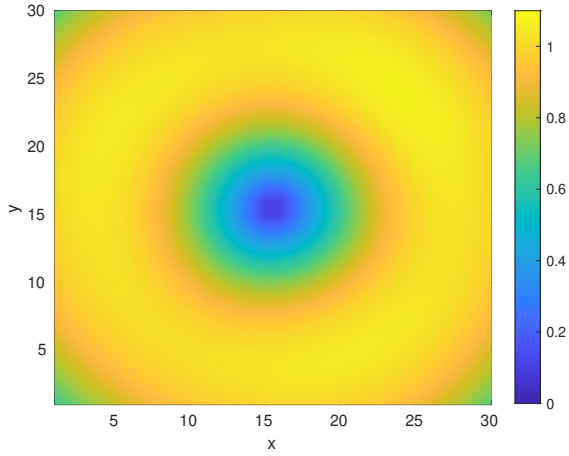

$T = 1, \varepsilon = 10^{-2}$

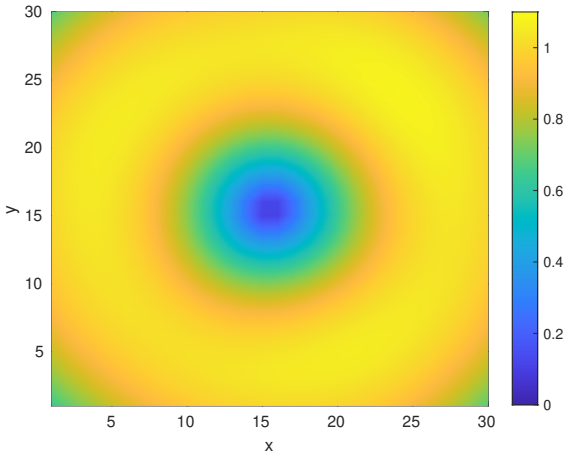

$T = 1, \varepsilon = 10^{-3}$

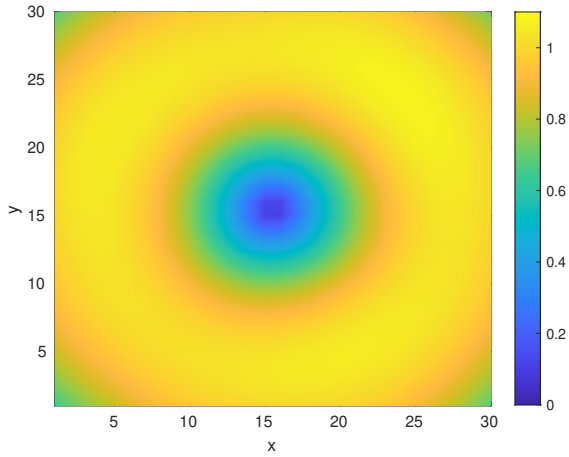

$T = 1, \varepsilon = 10^{-4}$

FIGURE 13. Steady vortex: the velocity $q = \sqrt{u^2 + v^2}$ initially and at the final time for different values of ε on 32 x 32 grid points.